Food Hydrocolloids 170 (2026) 111693

Contents lists available at ScienceDirect

Food Hydrocolloids

journal homepage: www.elsevier.com/locate/foodhyd

Development of alginate-based active edible coating with *Brassica juncea* and *Raphanus sativus* sprout extracts to extend tomato shelf-life

Arash Moeini [a,*], Sarai Agustin Salazar [b], Luca Gargiulo [b], Roméo Arago Dougué Kentsop [c], Monica Mattana [c], Annamaria Genga [c], Christin Josi [a,d], Parisa Pedram [a], Gustavo Cabrera-Barjas [e], Simona Guerra [f], Massimiliano Marvasi [f], Thomas Becker [a], Pierfrancesco Cerruti [b]

[a] Chair of Brewing and Beverage Technology, TUM School of Life Sciences, Technical University of Munich, 85354, Freising, Germany
[b] Institute of Polymers, Composites and Biomaterials (CNR-IPCB), Via Campi Flegrei 34, 80078, Pozzuoli, Italy
[c] Institute of Agricultural Biology and Biotechnology, National Research Council, 20133, IBBA, Milan, Italy
[d] Chair for Biogenic Polymers, Technische Universität München, 94315, Straubing, Germany
[e] Facultad de Ciencias para el Cuidado de la Salud, Universidad San Sebastián, Concepción, Biobío, Chile
[f] Department of Biology, University of Florence, Via Madonna del Piano 6, 50019, Sesto Fiorentino (FI), Italy

ARTICLE INFO

Keywords:
Active edible coating
Alginate
Antimicrobial
Antioxidant
Shelf life
Essential oil

ABSTRACT

Extending the shelf life of fresh produce using sustainable, bio-based preservation methods is an exciting and rapidly growing area of research, driven by the need to reduce food waste and meet consumer demand for chemical-free alternatives. This study presents the development of an alginate-based active edible coating incorporating *Brassica juncea* (GM) and *Raphanus sativus* (RT) sprout extracts to prolong tomato shelf life. The coating was prepared by modifying glycerol-plasticized alginate (A) with zein/chitosan (Z/CH) microparticles (MPs) containing the sprout extracts as bioactive antimicrobial and antioxidant agents. The physicochemical properties of the films were characterized using FTIR, SEM, TGA/DSC, contact angle, water vapor permeability, and tensile testing. FTIR analysis revealed interactions between alginate and MPs, TGA confirmed thermal stability, SEM showed uniform MP dispersion, and tensile tests indicated improved flexibility with extract addition, enhancing coating suitability. Encapsulated extracts increased antioxidant activity, achieving 52 % DPPH inhibition for GM and 70 % for RT. The antimicrobial assay demonstrated that RT-formulated films showed moderate biocidal activity against *Bacillus cereus* and *Salmonella enterica*, highlighting their potential to improve food safety. Furthermore, tomato shelf-life testing revealed a 30-day extension using RT-loaded MPs, with no visible changes in appearance or texture. These findings suggest that encapsulating RT in plasticized alginate coatings enhances tomato longevity and quality, supporting the use of edible films for active food packaging applications.

1. Introduction

Non-biodegradable polymers such as polyethylene terephthalate, high- and low-density polyethylene, polyvinyl chloride, polypropylene, and polystyrene provide excellent protection against food deterioration and physical damage. However, their widespread use has resulted in severe environmental consequences (Moeini et al., 2021; Risch, 2009). Despite growing awareness, only one-third of plastic is estimated to be recycled (Schwarzböck et al., 2016), highlighting the inefficiency of current waste management systems.

This pressing issue underscores the urgent need for more sustainable and biodegradable alternatives to fossil-based polymers, particularly in the food packaging industry. This is why, by 2030, the European Sustainable Development Goals aim to expand the use of bio-based and biodegradable bioplastics while reducing plastic pollution (Communication from the commission to the European parliament, the council, the European Economic and social committee and the committee of the regions Closing the loop - An EU action plan for the Circular Economy, 2015). Generally, biopolymers have low gas permeability, which is highly desirable for food packaging applications, although

* Corresponding author.
E-mail address: arash.moeini@tum.de (A. Moeini).

https://doi.org/10.1016/j.foodhyd.2025.111693
Received 7 April 2025; Received in revised form 14 June 2025; Accepted 21 June 2025
Available online 27 June 2025

these gas barrier properties are lowered by adding plasticizers or moisture. Recently, there has been an increased demand for biopolymers as edible coatings. Edible coatings help protect food from microbial contamination by providing effective gas barriers and enhancing mechanical properties, thereby extending the food's shelf life. Furthermore, they improve coated meals' organoleptic and sensory qualities (Valdés et al., 2014). Recently, there has been an increased demand for biopolymers as edible coatings, especially for protecting perishable food. Polysaccharides, proteins, and lipids are the most common edible biopolymers in food coatings. These biopolymers are low-cost, industrially scalable, biodegradable, and biocompatible, making them ideal for delivering antioxidant and antibacterial compounds that enhance food safety (Horita et al., 2018). Chitosan (CH) and alginate (A) are among the most researched polysaccharides for edible films. CH is the polymer of poly N-acetyl-glucosamine and N-glucosamine, and is obtained from chitin via N-deacetylation. Shrimp shells, lobsters, crab peritrophic membranes, and insect cocoons are the main sources of chitin. Remarkably, the U.S. Food and Drug Administration (FDA) approved chitosan's edibility in 2001, which led to a rise in its use in the food business (Moeini, Pedram, et al., 2020; No et al., 2007). Meng et al. demonstrated that pre-harvest application of edible chitosan coatings effectively inhibited the growth of pathogenic bacteria and reduced spoilage, thereby improving the shelf life and quality of fruit after harvest (Meng et al., 2008). In another study, edible chitosan covering before and after harvest extended the fruit's shelf life before and during cold storage (Chien et al., 2007). Alginate, a linear (1 → 4) linked polyuronic acid (anionic polysaccharide) found in seaweed, is also used in edible coatings for food packaging (Giannakas et al., 2022, 2023; Meseldzija et al., 2024; Nesic et al., 2020).The mechanical and physicochemical properties of alginate edible films are determined by the polyvalent cations, pH, temperature, and material formulation, which can be modified with plasticizers and emulsifiers or blended with other polymers. Alginate films have excellent tensile strength (TS), flexibility, tear resistance (TR), and stiffness (Di Donato et al., 2020). Like other edible polysaccharides, alginate films are tasteless, grease-resistant, glossy, and odorless (Theagarajan et al., 2019). Corn zein (Z) is an aqueous alcohol-soluble protein, except for high- and low-pH, and insoluble in pure alcohol (Sahraee et al., 2019). As a result, corn zein cast films are produced using a temperature-controlled solution of aqueous ethyl alcohol or isopropanol. During solvent evaporation, the zein chains form hydrophobic, hydrogen, and disulfide linkages, producing mechanically stable films (Mayer et al., 2021; Padua & Wang, 2002). Developing edible coatings is one of the most prominent applications for these film-forming biopolymers in food packaging. In this procedure, a thin layer of edible polymer coats the food's surface, protecting it from oxidation, dampness, microbial development, and degradation. Furthermore, edible coating materials have demonstrated gas, vapor, and oil barrier qualities and may be employed as carriers for active agents. Bioactive molecules that can function as antioxidants, antimicrobials, and plasticizing agents can be included in the packaging system to create active packaging (Moeini, 2020), increasing food quality and extending shelf life (Garcia et al., 2014). This technology has superseded traditional food preservation methods for preventing food degradation by surface interactions with food products or altering the headspace between the food and the packaging surface. This innovative packaging strategy employs biofunctional chemicals as active agents (Nguyen Van Long et al., 2016). Furthermore, there is a growing trend to exploit plant-derived natural compounds, such as secondary metabolites, which has led to applying natural, secondary compounds as additives in active packaging (Granato et al., 2017; Vinceković et al., 2017). Secondary substances include natural metabolites and essential oils extracted from plants and fungi (Ioannou & Roussis, 2009; Johnson et al., 2018), which can be integrated into packing systems to prevent food and texture changes. In this regard, Mohammadi et al. demonstrated cinnamon EO antibacterial efficacy against *E. coli, S. aureus*, and *S. fluorescence* by incorporating it into chitosan nanofiber and whey protein films for active packaging (Mohammadi et al., 2020). Lindi et al. reported using rosemary essential oil in Fenugreek seed mucilage-based active edible coating films, extending apples' shelf life by 30 days (Lindi et al., 2024).

Green Mustard (GM) (*Brassica juncea*) and Red Tango Radish (RT) (*Raphanus sativus*) Lettuce belong to the same family of edible leafy greens. GM belongs to the Brassica genus and originates in Central Asia (Szőllősi, 2020). RT is a root vegetable from the Brassicaceae family, which includes cabbage, broccoli, and mustard. It is extensively grown for its edible root and originates in Southeast Asia or the Mediterranean region (Goyeneche et al., 2015).

RT and GM sprouts contain important phytochemicals such as phenolics, flavonoids, anthocyanins, and isothiocyanates. These chemicals have a variety of biological properties, including anti-inflammatory, anticancer, and antioxidant (Goyeneche et al., 2015; Szőllősi, 2020). Aside from their health benefits, these compounds derived from RT and GM may be useful as natural antioxidants/antimicrobials for edible film coating or packaging (Mohan et al., 2023).

Based on these considerations, in this study, we report on developing a novel active edible coating film by formulating GM and RT extracts as antioxidant agents into alginate films. For this purpose, GM and RT are first encapsulated into Z/CH microparticles (MP), and then formulated in an alginate polymer matrix to yield composite films. The effect of the MPs on the films was investigated using TGA, FTIR, contact angle, and water vapor permeability tests. Tensile tests and SEM analysis were also employed to assess the films' mechanical performance, morphology, and distribution of the MP. The antioxidant and antimicrobial activity of RT and GM were then determined and validated by performing shelf-life tests on coated tomato fruits.

2. Material and methods

2.1. Materials

Zein, chitosan high molecular weight (CH_{HMW}, 310–375 kDa and deacetylation degree 75 %), chitosan low molecular weight (CH_{LMW}, 150–500 kDa, and deacetylation degree 75 %), Tween 20, polyvinyl alcohol (PVA) (molecular weight 2000 kDa), pectin from apples (10–300 kDa) with the Degree of Esterification of 50–75 % and galacturonic acid of 75–80 %, low viscosity Alginic acid sodium salt from brown algae with M/G ratio of 1.56 and Molecular weight of 30–100 kDa, ethanol, and acetic acid were purchased from Sigma-Aldrich (Milan, Italy). Tomatoes were bought from the local supermarket.

2.2. Preparation of RT and GM extracts, microparticles, and edible coating formulation

RT and GM seeds were sprouted in vessels at 22 °C in the dark, and water was sprayed twice daily. After 5 days, RT and GM sprouts were harvested, immediately frozen, finely grounded, and freeze-dried. The extraction was performed with 120 ml of 80 % ethanol per 1 g of dry sample, sonicated for 30 min, and left O.N. under magnetic stirring at room temperature. The samples were filtered and dried under a rotavapor. The remaining aqueous residues were freeze-dried and stored at −20 °C until used.

RT and GM sprout extracts were encapsulated in MPs, as described in our previous study (Aspen, 2024). Briefly, zein (Z) (2.0 % w/v), chitosan (CH) (0.5 % w/v), and Tween 20 (10 % v/v) solutions were prepared. RT and GM (6 % w/w) were added to the Z solutions and stirred for 30 min based on the Z weight. After this, the appropriate amount of CH was added with two different proportions of Z:CH (5:1), and stirring continued for 30 min. Finally, T (10 % v/v) was added, and stirring continued for another 30 min. The formulated samples are labeled Z/CH/RT and Z/CH/GM.

The RT and GM encapsulated, and blank MPs dispersions were formulated into Alginate (A), CH_{HMW}, and PVA matrices as a dispersing

phase and thickening agent to create edible films for tomato coating. For this purpose, PVA (1 % w/v) and A (2 % w/v) solutions were dissolved in distilled water, and CH_{HMW} (1 % w/v) was dissolved in acetic acid (1 % v/v). Both PVA and CH_{HMW} were vacuum-filtered. Different glycerol concentrations were also introduced as plasticizers. The homogenized solutions were then used to coat tomatoes and poured into a Petri dish to cast.

Glycerol (G) (10 % or 20 % w/w) was first added to A (2 %) and stirred for 3 h to prepare the formulated coating films. Then, the already prepared Z/CH/RT, Z/CH/GM, and blank MPs solution were individually added to A solution with a biopolymer matrix: MP (v:v) ratios 1:1 and homogenized using a homogenizer (the Ultra Turrax T50, Ika Werke) for 5 min in an ice bath and kept under stirring overnight. After stirring, these mixtures were used for the coating, cast into the 9 cm diameter plastic Petri dish, and let dry under a hood at room temperature for 48 h. Then, the films were further used to study physicochemical characterizations. A similar protocol is followed for PVA and CH_{HMW}. The coating films are Z/CH/RT or GM: A/G (10 or 20), PVA, and CH_{HMW}.

2.3. Physicochemical characterizations

2.3.1. Fourier-transform infrared spectroscopy (FTIR)

Infrared analysis was conducted on the film surfaces using a Spectrum 3 Tri-Range MIR/NIR/FIR Spectrometer (PerkinElmer, Waltham, MA, USA) equipped with a Universal ATR diamond crystal sampling accessory. Spectra were recorded as an average of 16 scans (range: 4000–650 cm^{-1}, resolution: 4 cm^{-1}).

2.3.2. Thermal analysis

Thermogravimetric analysis (TGA) was performed under a nitrogen atmosphere (flow rate 100 mL min−1) using a 7.5 ± 2.0 mg sample by means of a PerkinElmer Pyris Diamond TG-DTA. The thermal program used was 30–100 °C (20 °C min^{-1}), 30 min isotherm, and heating up to 700 °C (10 °C min^{-1}) (Aspen, 2024).

Differential Scanning Calorimetry analyses (DSC) were performed with a TA DSC-Q2000 instrument under a 50 mL min^{-1} nitrogen flow. Samples (4.0 ± 2.0 mg) were first heated from −70 to 180 °C at 10 °C min^{-1}, then cooled down to −70 °C at 10 °C min^{-1} and reheated up to 200 °C at 10 °C min^{-1}.

2.3.3. Scanning electron Microscopy (SEM)

Film samples of about 1 × 2 cm^2 were frozen by immersion in liquid nitrogen for 5 min, then freeze-fractured. The samples were coated with an Au/Pd layer to increase conductivity. The fractured cross-section was then analyzed using an FEI Quanta 200 FEG microscope (FEI Company, OR, USA) SEM to examine morphological features of the cryo-fractured surface. An accelerating voltage of 10 kV and a secondary electron detector were used (Aspen, 2024).

2.3.4. Water contact angle

Contact angle (θ) was measured to assess the wettability of the surfaces by measuring the Static contact angle measurements obtained by the drop shape analysis using a Micro-Drop® (First Ten Angstroms Inc., Italy) contact angle meter with a high-speed framing camera. Uniform drops of deionized water (3 μL) were placed on a horizontal film surface with a syringe at room temperature. The contact angle was evaluated using FTA1000 Manual Drop Shape Analysis Software 2.0 version (FTA Inc. Portsmouth, VA, USA) from the drop shape by measuring the angle formed between the substrate surface and the tangent drawn from the edge of the drop. The contact angle values are reported as an average of 3 measurements (Agustin-Salazar et al., 2024a).

2.3.5. Water vapor barrier properties

The water vapor transmission rate (WVTR) of the films was determined using the "cup method" according to ASTM ISO 7783 (ASTM, 2014), with some modifications. A cylindrical aluminum vessel was filled with calcium chloride (4.5 ± 0.5 g), and the top opening was sealed with the studied film. The aluminum vessels were kept in a chamber set at 25 °C with a relative humidity of 50 % until reaching the equilibrium conditions. The weight change of the cell was measured every 24 h. Each sample was tested in triplicate to confirm the repeatability of measurements (Agustin-Salazar et al., 2024a).

2.3.6. Tensile properties

Tensile tests were performed on dog bone-shaped film cutouts (gauge length and width: 20 × 0.4 mm^2, thickness values are reported in Table 2). Tests were carried out by using an Instron model 5564 dynamometer (U.S.A.) equipped with a 1 kN load cell at 23 ± 2 °C, 45 ± 5 % RH, with a 5 mm min^{-1} clamp separation rate (Agustin-Salazar et al., 2017). The experimental data is an average of 5 determinations. Before testing, the samples were conditioned at 25 °C, 50 % RH for 5 days.

2.3.7. Statistical analysis

FTIR peak wavenumber values for FT-IR were calculated and obtained through the Origin Pro software (Origin-Lab Corporation, Northampton, MA, USA) peak analyzer. The pH, loading efficiency, and contact angle values were calculated using Excel as means ± standard deviations (Microsoft Corporation, 2018). All the experimental data were evaluated using a one-way analysis of variance (ANOVA) using R software (version 4.3.2 for Windows) with a significance level of $p < 0.05$. Tukey's Honest Significant Difference (HDS) test tested significant differences among the means.

2.4. Biological assay

2.4.1. Antioxidant assay of films

Antioxidant activity was performed on formulated alginate films uncoated and coated with unloaded and loaded RT and GM microparticles. The antioxidant activity was determined through DPPH assay according to the method described by Moccia et al., 2020 with slight modification (Moccia et al., 2020). Specifically, a section of 1 cm^2 film was cut, weighed, and immersed in a test tube containing 3 ml of 101.4 μM ethanolic solution of 2,2-diphenyl-1-picrylhydrazyl (DPPH). The absorbance of the samples was read at 515 nm with a JascoV730 UV–Vis spectrophotometer during a time course starting after 30 min, 1, 2, 4, 6, 24, 48, 72, 96, and 168 h (A1). A test tube containing DPPH solution without film was prepared and used as a Blank for each time point (A0). The antioxidant activity was expressed as a %inhibition of DPPH per cm^2 of film. Each experiment was performed at least in triplicate.

- $\%\ inhibition\ of\ DPPH = ((A0-A1)/A0)\times 100/cm^2\ film$

The EC 50 was determined for RT and GM extracts by preparing different concentrations of the two extracts, and ascorbic acid was used as a positive control.

2.4.2. Antimicrobial assay

Salmonella enterica serovar *Typhimurium* strain 19585 and *Bacillus cereus* ATCC10987 were used to assess the biocidal activity of the coatings. Overnight cultures of *S. Typhimurium* and *B. cereus* were grown in Tryptic Soy Broth (VWR) at 37 °C, under constant agitation at 200 r.p.m. for 18 h. Following incubation, the bacterial cultures were serially diluted in physiological saline solution (0.8 % NaCl w/v) to achieve a concentration of approximately 1 × 10^6 CFU/mL. A 20 μL aliquot of the bacterial suspension was carefully applied onto circular coupons (radius: 1.5 cm) of various formulations films (A/G10 or G20), and films modified with unloaded MPs (Z/CH:A/G10 or G20) and loaded MPs (Z/CH/GM:A/G10 or G20, Z/CH/RT:A/G10 or G20). Polyethylene terephthalate (PET) was used as a control. The coupons with the bacterial inoculum were incubated at 4 °C for 24 h to simulate contamination during refrigeration. After incubation, each coupon was transferred into

Table 1
Thermal parameters obtained from TGA and DSC of the films including alginate (A) and glycerol (G), green mustard (GM), red radish (RT), and microparticles (MPs) based on chitosan (CH) and zein (Z). For all values with the same letter, the difference between the means is not statistically significant.

Sample code	DSC			TGA				
	H_2O evaporation peak °C	H_2O evaporation enthalpy J/g	Zein T_g °C	Moisture %	T_{onset} °C	T_{max1} °C	T_{max2} °C	Char yield %
A/G10	88.9 ± 1.0^{b}	718.9 ± 5.9^{g}	–	21.2 ± 1.1^{b}	201.0 ± 1.1^{c}	216.2 ± 2.1^{a}		41.9 ± 4.8^{g}
A/G20	112.8 ± 0.8^{d}	686.0 ± 4.8^{f}	–	17.4 ± 1.0^{a}	199.5 ± 2.0^{c}	215.4 ± 0.9^{a}		35.9 ± 6.2^{g}
Z/CH:A/G10	93.7 ± 1.3^{c}	558.6 ± 4.4^{e}	40.0 ± 2.3^{d}	22.5 ± 1.4^{b}	208.3 ± 1.8^{d}	234.1 ± 0.8^{a}	356.8 ± 1.2^{a}	27.2 ± 3.6^{e,f}
Z/CH:A/G20	122.3 ± 1.3^{e,f}	401.9 ± 5.3^{b}	35.1 ± 3.1^{c}	30.3 ± 3.1^{g}	200.1 ± 2.0^{c}	236.6 ± 1.3^{b}	379.2 ± 0.7^{d}	10.5 ± 2.5^{b}
Z/CH/GM:A/G10	120.1 ± 1.0^{e}	428.2 ± 6.1^{c}	34.1 ± 2.0^{c}	18.1 ± 1.7^{a}	201.9 ± 3.1^{c}	233.2 ± 1.5^{a}	368.3 ± 2.3^{b}	21.1 ± 4.1^{d,e}
Z/CH/GM:A/G20	123.6 ± 1.2^{f}	417.3 ± 5.0^{c}	24.1 ± 1.7^{a}	18.5 ± 1.2^{a}	195.8 ± 1.1^{b}	235.2 ± 3.0^{a,b}	373.8 ± 2.5^{c}	19.2 ± 3.8^{c,d}
Z/CH/RT:A/G10	I)83.0 ± 0.7^{a} II)128.0 ± 1.5^{g}	458.9 ± 4.7^{d}	28.2 ± 2.1^{b}	25.3 ± 2.1^{b}	192.6 ± 1.0^{a}	234.5 ± 1.9^{a,b}	367.3 ± 2.0^{a,b}	5.5 ± 2.4^{a}
Z/CH/RT:A/G20	122.8 ± 1.0^{f}	330.4 ± 2.3^{a}	27.4 ± 1.9^{a,b}	24.1 ± 1.8^{b}	194.0 ± 2.1^{a,b}	237.5 ± 0.9^{b}	372.1 ± 1.1^{c}	13.8 ± 2.7^{b,c}

Table 2
Thickness, mechanical, and water vapor barrier properties of the alginate-based films including alginate (A) and glycerol (G), green mustard (GM), red radish (RT), and microparticles (MPs) based on chitosan (CH) and zein (Z). For all values with the same letter, the difference between the means is not statistically significant.

Sample	Thickness	Strain at break	Elastic Modulus	Ultimate Strength	WVP
	mm	%	MPa	MPa	g m^{-1} Pa^{-1} s^{-1} x 10^{-10}
A/G10	40.5 ± 2.3^{a}	6.1 ± 1.1^{b}	2018 ± 640^{d}	30.5 ± 5.3^{c}	1.87 ± 0.73^{a}
A/G20	36.6 ± 1.8^{a}	4.8 ± 2.2^{a,b}	1005 ± 419^{d}	13.8 ± 3.3^{b}	1.43 ± 0.03^{b,}
Z/CH:A/G10	59.2 ± 3.0^{d}	5.4 ± 3.0^{a,b}	222 ± 90^{b,c}	3.1 ± 0.5^{a}	–
Z/CH:A/G20	48.4 ± 2.3^{b}	8.5 ± 4.3^{b,c}	195 ± 28^{b}	3.3 ± 0.7^{a}	1.50 ± 0.13^{b,c}
Z/CH/RT:A/G10	52.1 ± 2.3^{b,c}	3.0 ± 0.8^{a}	237 ± 55^{b,c}	2.9 ± 1.5^{a}	1.63 ± 0.05^{c}
Z/CH/RT:A/G20	57.6 ± 2.7^{d}	3.9 ± 1.8^{a,b}	320 ± 120^{b}	4.5 ± 1.4^{a}	1.26 ± 0.11^{a}
Z/CH/GM:A/G10	54.6 ± 2.6^{c,d}	4.6 ± 1.2^{a,b}	290 ± 60^{c}	3.8 ± 0.9^{a}	1.39 ± 0.16^{a,b}
Z/CH/GM:A/G20	59.4 ± 2.9^{d}	12.8 ± 5.2^{c}	104 ± 20^{a}	2.7 ± 0.3^{a}	1.67 ± 0.08^{c}

a 1.5 mL tube containing 1 mL of Phosphate Buffered Saline (PBS, VWR), vortexed at maximum speed for 60 s, and 50 μL of the resulting suspension was plated onto Xylose Lysine Deoxycholate (XLD, OXOID) agar plates for selective enumeration of *Salmonella* Colony Forming Units (CFUs) and on Chromatic *Bacillus cereus* agar (VWR). A total of six replicas were performed.

The antimicrobial activity of the coatings was also evaluated using the agar diffusion method. *S. Typhimurium* strain 19585, inoculated overnight as previously described, was diluted in Phosphate Buffered Saline (PBS) to match the turbidity of a 0.5 McFarland standard. A 100 μL aliquot of the bacterial suspension was spread evenly onto Tryptic Soy Agar (TSA, VWR) plates to create a uniform bacterial layer. For control purposes, three antibiotic discs soaked with 20 μL of 5 mg/mL tetracycline were placed onto the surface of one bacterial layer. In the experimental setup, three circular discs (0.5 cm in diameter) of each coating were placed on the bacterial layer of separate plates. Each Petri dish contained a single type of coating. Plates were incubated statically at 37 °C for 18 h, after which the inhibition zones around the discs were measured with a ruler.

2.4.3. Application of developed Films for the durability Assessment of fresh cherry tomatoes

The shelf-life analysis of the coated and uncoated (control) cherry tomatoes was performed. The tomatoes were washed and dried. Next, the dip coating procedure was as follows: the fruits were submerged entirely in the filmogenic solutions for 1 min and then drained for 2–3 min, using nylon screens to eliminate excess solutions. Then, the covered fruits were placed at RT for 60 min under the hood to dry. After drying, the coated tomatoes were placed in a Petri dish in the dark conditions at room temperature. The shelf-life analysis of the coated and uncoated tomatoes was carried out. The sensory quality was evaluated by color, damage, texture, and overall acceptability for all the samples during storage.

The biological weight loss of tomatoes was carried out by taking mass measurements every two days. The tomatoes are weighed three times, and the mass loss is calculated from the averages obtained with the following formula:

$$Diff(\%) = \frac{m_{D0} - m_{Dx}}{m_{D0}} \times 100 \quad (2)$$

m_{D0}: mass on day 0
m_{Dx}: mass on the day of calculation.

3. Results and discussion

In previous work, a novel edible coating formulation based on RT and GM extracts was reported (Aspen, 2024), in which PVA and CH_{HMW} were applied as dispersing and thickening agents for formulating Z/CH/RT and Z/CH/GM MPs with optimized concentration and proportion, aimed to maximize antioxidant activity. Following that, in this work, A, PVA, and CH_{HMW} films were formulated by different proportions of the MPs containing 6 % w/v of RT and GM (3:1, 2:1, and 1:1) to produce active edible coating films (Fig. 1). Among them, films with a proportion of 1:1 showed the highest antioxidant activity and were considered for development in this study. For this purpose, to improve the film's mechanical performance and compatibility between the Z/CH MPs and polymer matrices, two different concentrations of glycerol were added to the biocomposite films as a plasticizer and compatible agents. In the next step, all the biocomposites films were used for coating the tomato to assess their functionalities. As shown in Fig. 2, PVA and CH_{HMW}-based films did not produce promising results as they could not extend the tomatoes' shelf life. Therefore, the work was continued with alginate-based biocomposites. Further characterization included

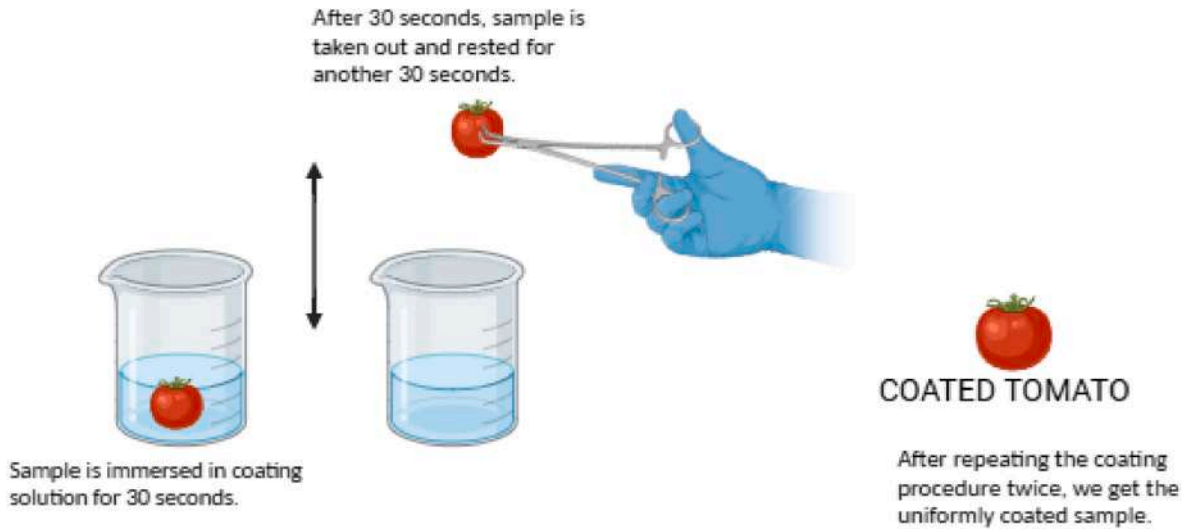

Fig. 1. Scheme of the protocol adopted to coat tomatoes with green mustard (GM) or red radish (RT) formulated alginate-based edible films. (For interpretation of the references to color in this figure legend, the reader is referred to the Web version of this article.)

physicochemical analyses such as FT-IR, SEM, TGA, wettability, permeability, and tensile strength tests. In addition, biological assays, including antimicrobial and antioxidant tests, were conducted. Finally, the functionality of the biocomposites was validated by conducting a shelf-life extension test on tomatoes.

3.1. Physicochemical analysis of alginate-based edible coating films

3.1.1. Fourier-transform infrared spectroscopy (FTIR)

The FTIR characterization provides relevant information on physical or chemical interactions between components in polymer-based formulations. The FTIR spectra of the alginate films, blank MPs, and GM and RT encapsulated MPs formulated films are shown in Fig. 3a.

The FTIR spectra of the blank sodium alginate showed the standard mannuronic acid functional group at 886 cm^{-1} and the uronic acid at 936 cm^{-1}, -OH functional group at 3200-3400 cm^{-1}, and CH_2 stretching at 2922 cm^{-1} (Derkach et al., 2020). In the curves, the C-O-C stretching vibration appears at 1025 cm^{-1}. The characteristic absorption peaks of the curves at 1595 cm^{-1}, 1410 cm^{-1}, 1297 cm^{-1}, and 950 cm^{-1} are related to asymmetric and symmetric COO^- group stretching vibrations, -C-O- stretch vibration, and the fingerprint of alginate (Bahraminejad et al., 2023; Li et al., 2021). To get insight into the effect of the content of glycerol on the film structure, the spectra of film samples containing 10 % glycerol were subtracted from the corresponding ones containing 20 % glycerol, as reported in Fig. 3b. The higher concentration of G in the alginate films resulted in significant increases of the peaks of carboxylate, hydroxy, and C-O-C groups in the films containing 20 % G. This phenomenon has been documented in previous studies, where increased glycerol concentrations in alginate-based films led to intensified O–H stretching (3200–3600 cm^{-1}), and COO^- stretching vibrations (1600 cm^{-1} and 1400 cm^{-1}) due to enhanced hydrogen bonding interactions (Gao et al., 2017; Jost et al., 2014). For instance, Jost et al. reported that higher glycerol levels amplified the O–H band intensity in alginate films, while Gao et al. noted changes in both O–H and COO^- bands, reflecting glycerol's interaction with alginate's functional groups (Gao et al., 2017; Jost et al., 2014).

The incorporation of Z/CH MPs into alginate films (Fig. 3a) leads to a shift in hydroxyl group peaks from 3250 cm^{-1} in A/Gly to 3280 cm^{-1} in A/Gly/MPs, which confirms the hydrogen bonding interaction between MPs and alginate polymer matrix. Besides, the formation of the peak around 1730 cm^{-1} is attributed to the ester bond, resulting from the crosslinking of zein and chitosan in MPs, and the increasing intensity of the peak at 1084 cm^{-1} is associated with the C-O stretching vibrations of carbohydrates, specifically the glycosidic bond of the MPs chitosan (Spasojević et al., 2019).

In Z/CH/RT and GM MPs incorporated films, the hydroxyl peak even shifted to a higher wavelength, which could confirm that the presence of RT and GM can affect hydrogen bonding and improve the incorporation of MPs into A/G films. In addition, the aliphatic C-H stretch resulting from RT and GM into the A/G films was observed at 2925-2923 cm^{-1} (Agustin-Salazar et al., 2024b).

3.1.2. Thermal analysis

3.1.2.1. Differential scanning calorimetry (DSC). DSC was used to analyze the thermal transitions, phase behavior, and intermolecular interactions in the biocomposite films. During the first heating scan of G10 samples, a broad endothermic peak centered at 90 °C (25–150 °C range) was observed, corresponding to the evaporation of loosely bound moisture (Fig. S1). This peak disappeared in the second scan, confirming the removal of free water. Films containing Z/CH MPs loaded with MG and RT exhibited an additional endothermic peak at 122–123 °C, attributed to the evaporation of tightly bound water associated with polymer chains (Liu et al., 2021). When glycerol content increased to 20 %, the broad low-temperature endotherm diminished in all MP-containing samples, while the high-temperature peak became dominant (Fig. 4a), indicating reduced moisture absorption.

This hydrophobization effect was corroborated by enthalpy measurements, as films with MPs and higher G content (e.g., Z/CH/RT:A/G20) showed ~50 % lower enthalpy values compared to blank alginate/glycerol (A/G) films, despite identical storage conditions (Table 1). This apparently odd result could be explained considering that higher glycerol levels may enhance polymer chain mobility, leading to a more compact or uniform film structure with reduced free volume or porosity (Gonçalves et al., 2019). A less porous film can limit water vapor penetration from the surrounding environment, contributing to lower moisture content. Additionally, glycerol's –OH groups compete with water for hydrogen-bonding sites on alginate. In this regard, Jost et al. found that as glycerol concentration increased (from 0 % to 75 % w/w based on alginate), the moisture content of the films decreased after drying and conditioning at 53 % relative humidity (RH) (Jost et al., 2014). At higher glycerol concentrations, stronger glycerol-alginate interactions may displace water molecules, reducing overall moisture retention. Additionally, MPs (Z/CH, Z/CH/RT, and GM) interact with the alginate matrix via hydrogen bonding (as confirmed by FTIR), restricting water uptake, a desirable trait for edible coatings to enhance

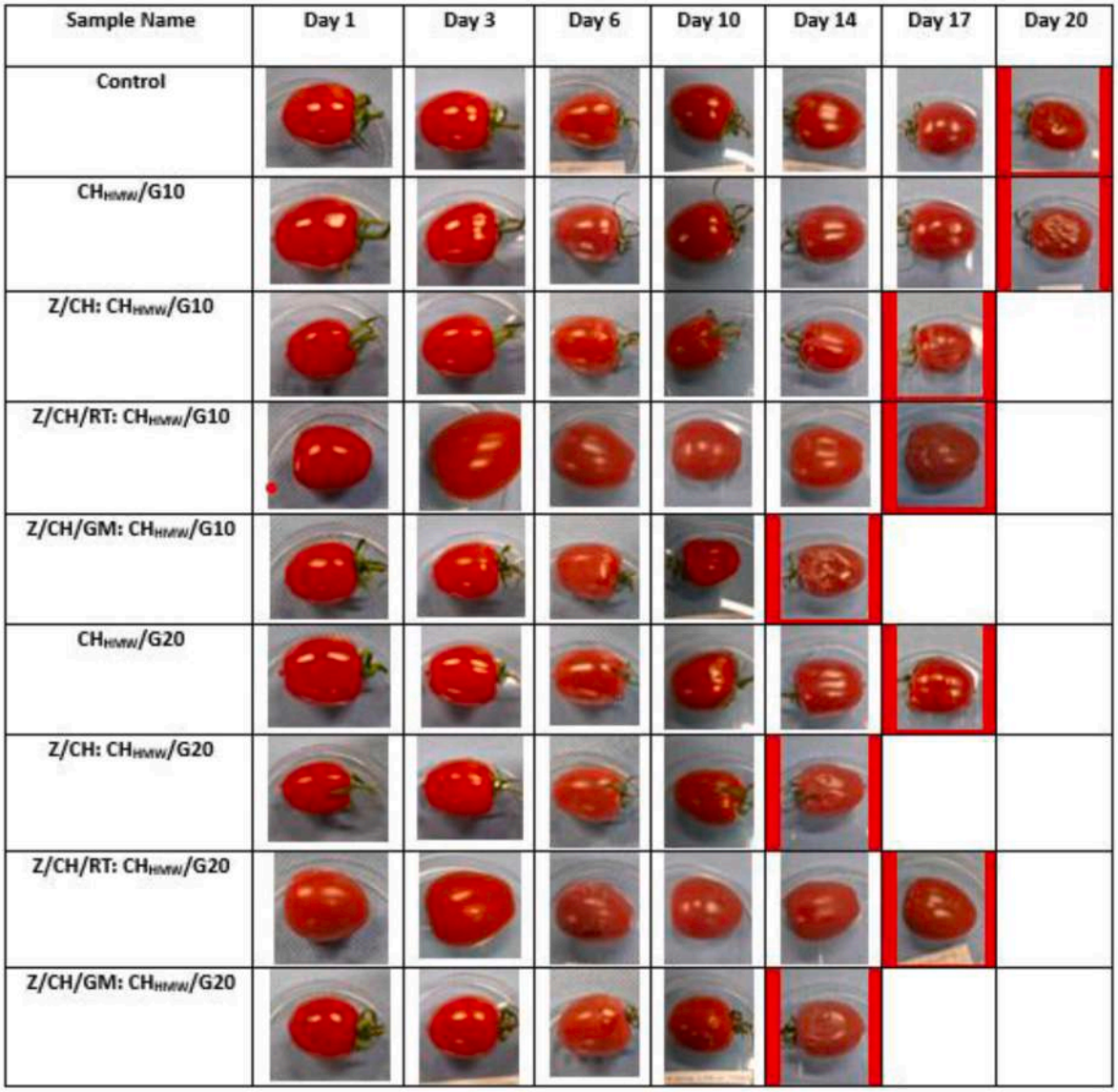

Fig. 2. Shelf-life extension test of cherry tomato coated with PVA/G, CH/G, RT, and GM-formulated MPs. The samples include Polyvinyl alcohol (PVA) and glycerol (G, 10 wt% or 20 wt%), green mustard (GM), red radish (RT), and microparticles (MPs) based on chitosan (CH) and Zein (Z). (For interpretation of the references to color in this figure legend, the reader is referred to the Web version of this article.)

shelf life (Paixão et al., 2019).

The second DSC scan revealed no significant thermal events, also for G20 film samples, confirming complete water evaporation and the absence of a glass transition (T_g) in neat alginate films (Fig. 4b). For the biocomposites, a melting transition of Tween 20 was detected near −10 °C, while weak Tg signals for zein appeared between 24 and 40 °C (Table 1) (Rojas-Lema et al., 2024).

3.1.2.2. Thermogravimetric analysis (TGA). TGA provides valuable insights into materials' thermal stability and degradation behavior. The thermal stability and decomposition behavior of alginate-based films were evaluated under a nitrogen atmosphere. The thermogravimetric curves are displayed in Fig. 5, and the thermal parameters calculated are summarized in Table 1. The films displayed distinct thermal parameters influenced by their composition, including moisture content, degradation onset temperature (T_{onset}), maximum degradation temperature (T_{max}), and char yield at 600 °C. As shown in Table 1, all films presented a moisture content above 15 %, confirming their hydrophilicity (Li et al., 2021). As glycerol concentration increased from G10 to G20, the moisture content generally decreased, except for the Z/CH:A samples, suggesting improved water resistance. However, the determination of the moisture content with TGA was not fully reliable. Indeed, as DSC showed especially in the case of A/G10 and A/G20, moisture evaporation began at temperatures as low as 25 °C, leading to an underestimation of the moisture content using thermogravimetry. Increasing glycerol concentration from 10 to 20 % generally reduced moisture content across formulations, except for Z/CH:A samples, indicating enhanced water resistance (Table 1), However, since DSC data for A/G10 and A/G20 films showed premature evaporation of free water at low temperatures (even lower than 25 °C), the moisture content evaluated by TGA in these samples was likely underestimated.

Including Z/CH MPs generally increased T_{onset}, as seen in Z/CH:A/G10 (208.33 °C) compared to A/G10 films (200.99 °C). This improvement is attributed to the thermal stability of chitosan and zein, which delays the thermal decomposition. However, T_{onset} reduction in RT and GM-formulated biocomposite films, such as Z/CH/GM:A/G20 and Z/

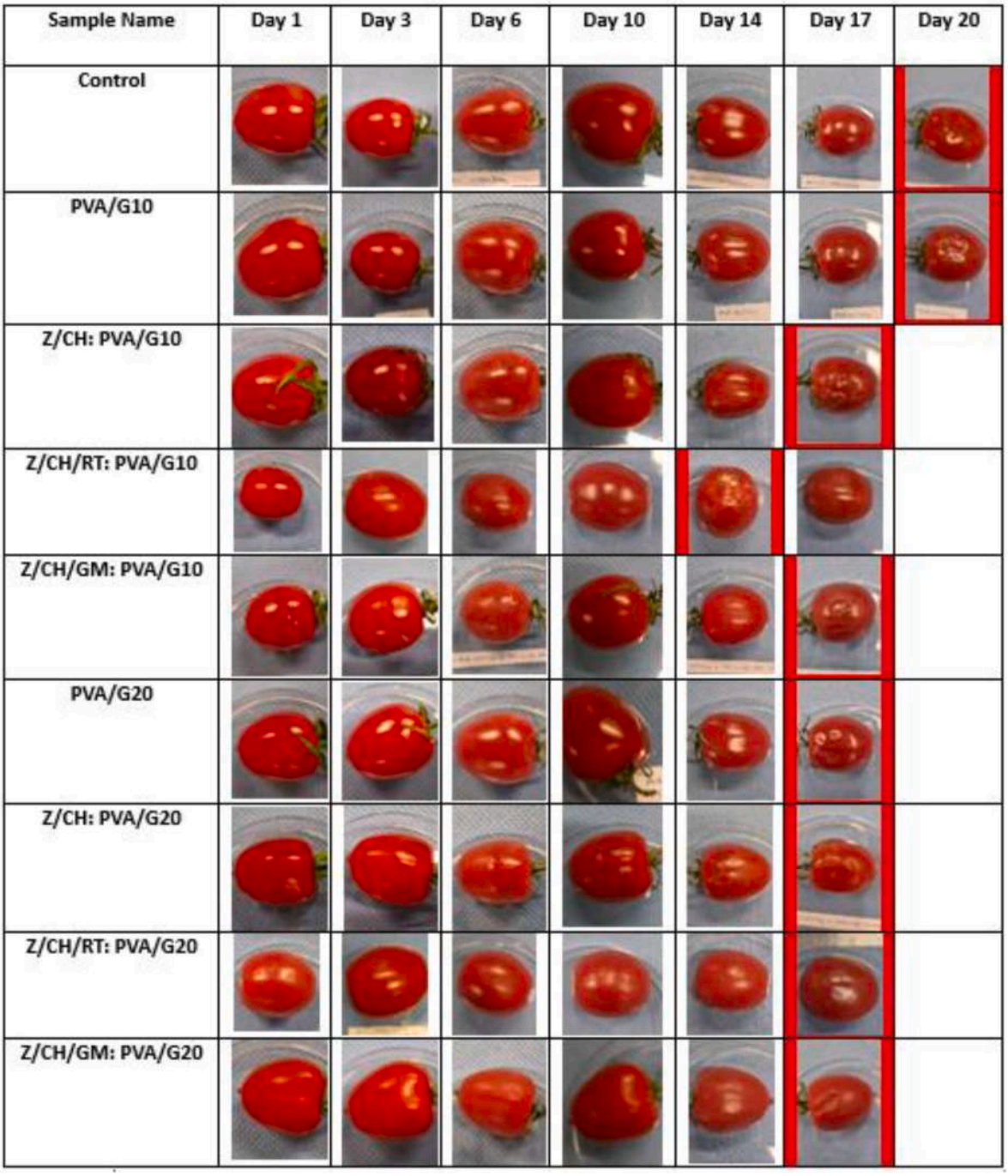

Fig. 2. (*continued*).

CH/RT:A/G20, indicated the presence of a volatile fraction in the RT and GM biomass. In A/G films, only one T_{max} was observed at about 215 °C, attributed to the degradation of the alginate chains, which shifted to a higher temperature of 233–237 °C in the biocomposites, reflecting the stabilizing effects of Z/CH MPs. However, Z/CH/GM:A/G and Z/CH/RT:A/G films that contained volatile components showed slightly lower T_{max} (I). The second T_{max} (II) occurred due to the breakdown of the Z/CH MPs network (Moeini et al., 2018). Biocomposite films containing RT and GM (Z/CH/GM:A/G and Z/CH/RT:A/G) showed significantly higher T_{max} (II) values (367–379 °C), which could be due to the successful encapsulation of RT and GM in Z/CH MPs that required higher temperatures for degradation (Moeini, Mallardo, et al., 2020; Moeini, van Reenen et al., 2020). Finally, the char yield of the biocomposites was lower than that of blank A/G films (41.9 % for A/G10 vs. 27.2 % for Z/CH:A/G10). Besides, adding RT and GM MPs could further decrease the yield, and the lowest yield was observed at A/G10/RT at 5.5 %.

3.1.3. Scanning electron microscopy (SEM)

SEM was used to analyze the morphology and the microstructure of the cross-section surfaces of films and biocomposites. As shown in Fig. 6, plain alginate films showed a smooth and rather uniform surface without visible agglomeration (Liu et al., 2021). The biocomposites displayed obviously rougher cross-section surfaces due to the presence of MPs, with the development of a distinct porosity observed in biocomposites compared to A/G films, attributed to the inclusion of Z/CH,

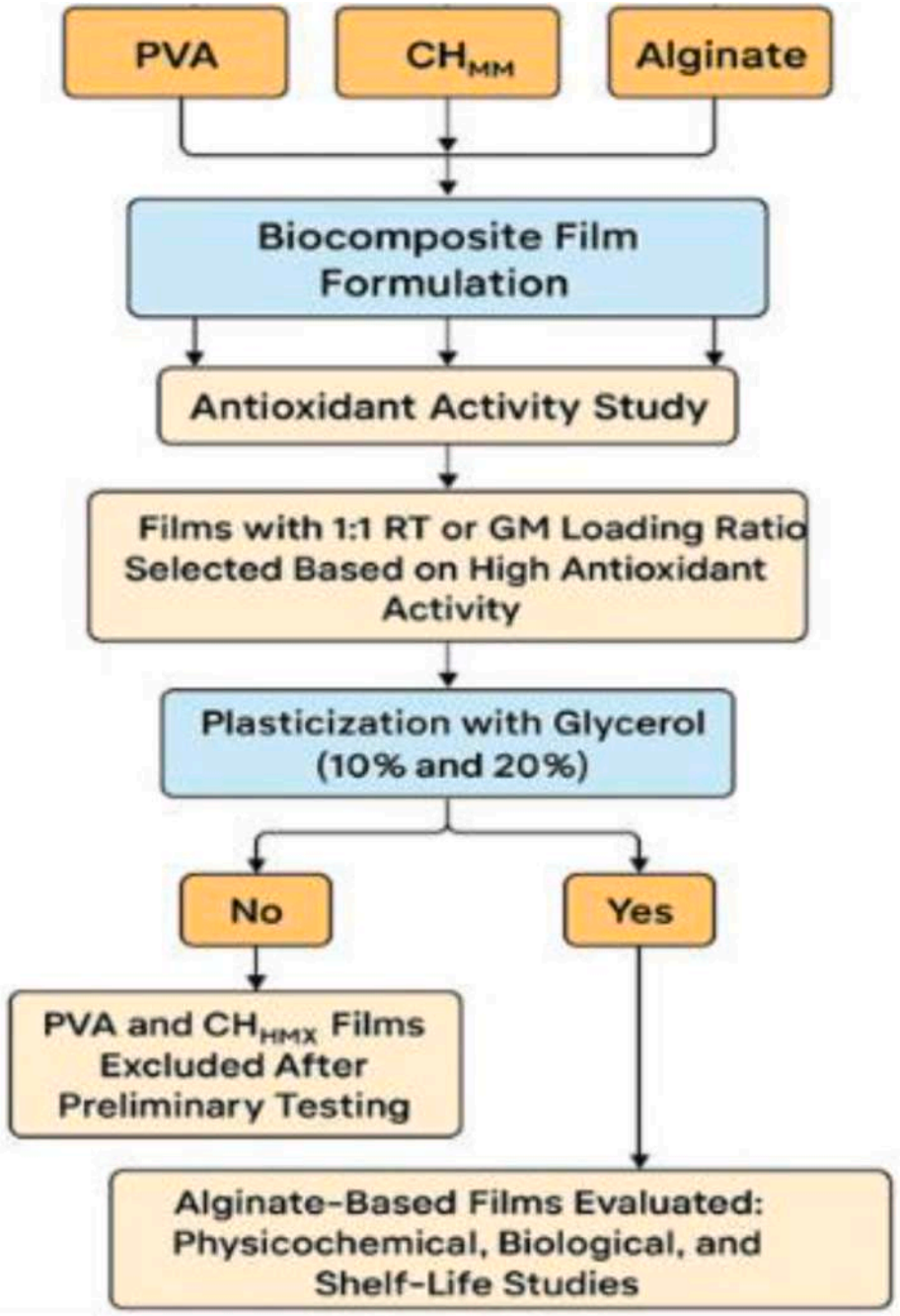

Schematic 1. Flowchart summarizing the development of edible films, from initial formulation with different matrices to selection of plasticized alginate-based coating films for final physicochemical, biological, and shelf-life evaluation.

Z/CH/RT, and GM microparticles in the alginate matrix (Moeini et al., 2018). These additives create structural heterogeneities and disrupt the compactness of the alginate-glycerol matrix. As already pointed out, the interaction between additive and polymer matrix reduces the tight packing of alginate chains, as the particles interfere with the polymer-polymer interactions, resulting in a less compact structure; therefore, the number of porosities increased (Moeini, 2020). Nonetheless, the rather homogenous appearance of the film cross sections confirms that Z/CH, Z/CH/RT, and GM microparticles are well embedded and evenly distributed into the A polymer matrix because of the strong interaction between MPs and alginate, as seen from FTIR, TGA, and DSC results.

3.1.4. Tensile properties

Tensile tests were used to evaluate the mechanical properties of the alginate-based films, including their strength, flexibility, stiffness, and elongation capacity, which are critical for determining the suitability of the films for packaging or coatings. In Fig. 7, representative stress-strain curves of all tested samples are shown, while the averaged relevant values obtained from the curves are reported in Table 2. Tensile test results reveal significant differences in the mechanical properties of alginate-based films depending on the glycerol content (10 % or 20 %) and the inclusion of Z/CH, Z/CH/RT, and GM MPs in the biocomposites. As expected, the biocomposites' thickness was higher with respect to the blank films, as the addition of MPs promoted the formation of voids. Strain at break decreased with increasing glycerol content, indicating that excess glycerol may weaken the film's cohesion and reduce the

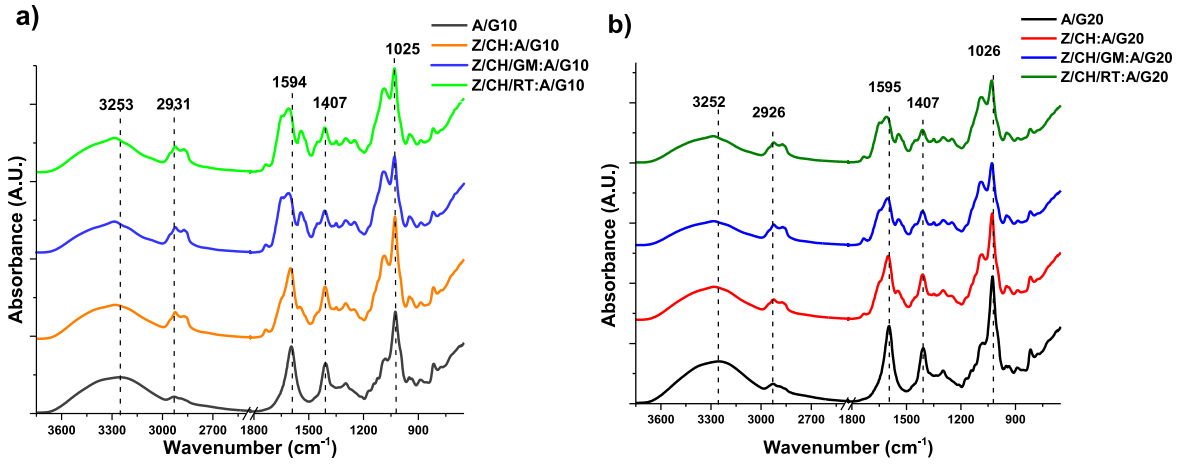

Fig. 3. a) FTIR spectra of the alginate-based films containing alginate (A), glycerol (G). green mustard (GM), red radish (RT), and microparticles (MPs) based on chitosan (CH) and zein (Z). b) Subtraction spectra of film samples containing 20 wt% and 10 wt% glycerol. (For interpretation of the references to color in this figure legend, the reader is referred to the Web version of this article.)

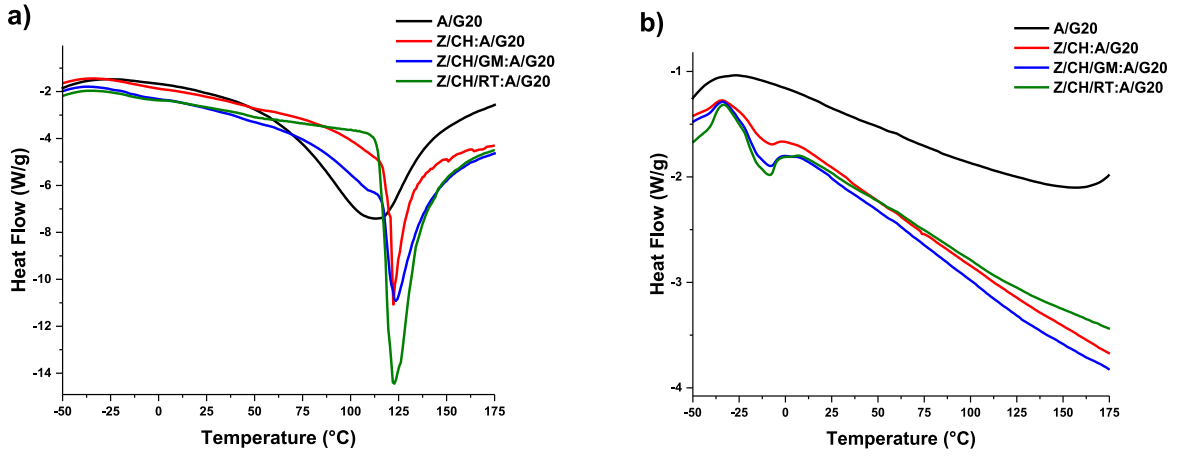

Fig. 4. DSC curves of the alginate-based films containing 20 wt% glycerol: a) first heating, and b) second heating. The samples include alginate (A) and glycerol (G), green mustard (GM), red radish (RT), and microparticles (MPs) based on chitosan (CH) and zein (Z). Endothermal signals are downwards. (For interpretation of the references to color in this figure legend, the reader is referred to the Web version of this article.)

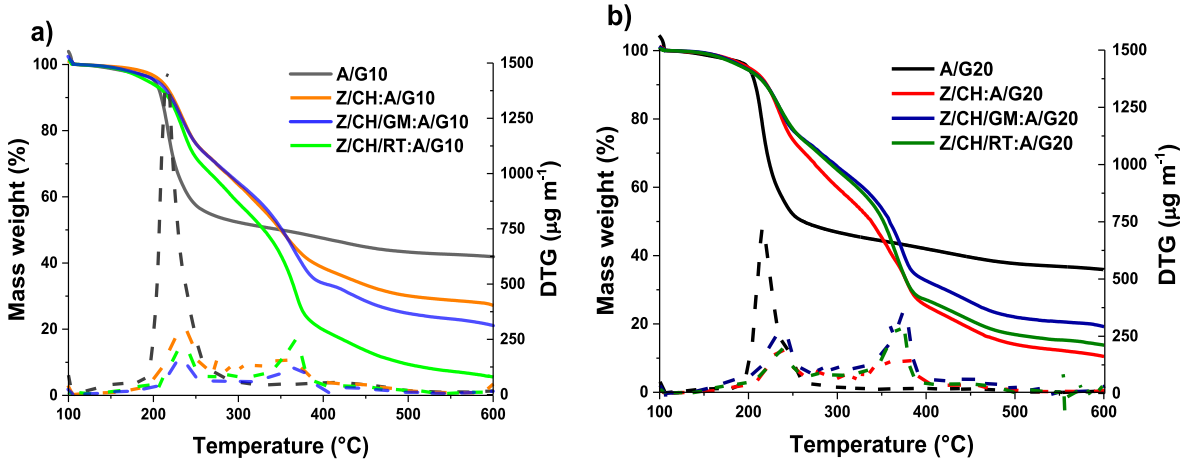

Fig. 5. TGA curves of the alginate-based films containing alginate (A) and glycerol (G), green mustard (GM), red radish (RT), and microparticles (MPs) based on chitosan (CH) and Zein (Z). a) 10 wt% glycerol, and b) 20 wt% glycerol. (For interpretation of the references to color in this figure legend, the reader is referred to the Web version of this article.)

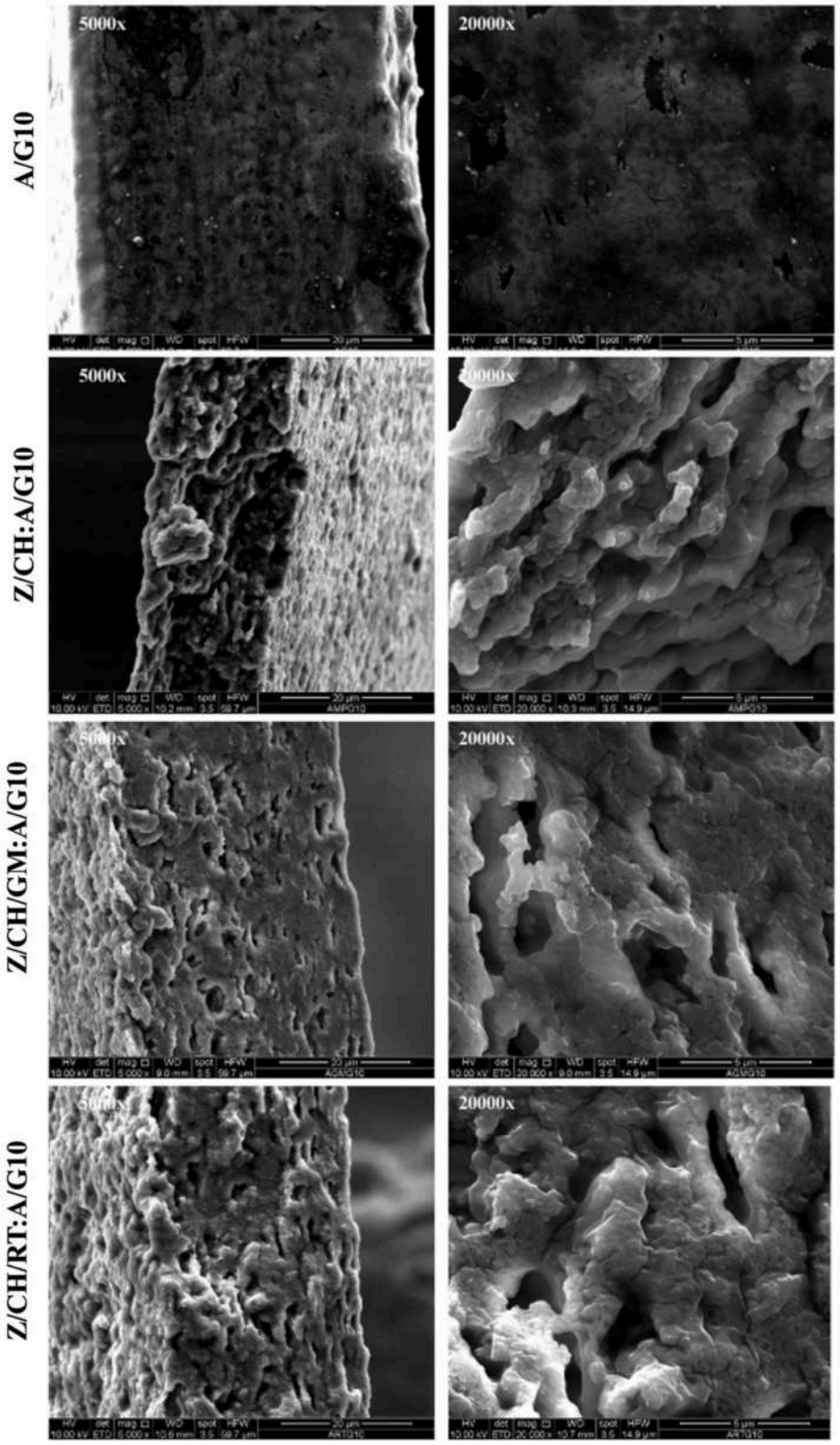

Fig. 6. SEM images of the alginate-based films with 10 % glycerol. Film samples include alginate (A) and glycerol (G), green mustard (GM), red radish (RT), and microparticles (MPs) based on chitosan (CH) and zein (Z).

ductility by disrupting polymer-polymer interactions. However, the strain at break in biocomposites with 20 % of G improved, and the most flexible film, with the highest strain at break, was Z/CH/GM:A/G20 (12.78 %). This could be due to the synergistic effect of glycerol and Z/CH MPs and the plasticizing effect of GM and their interaction with glycerol, which increased the elongation capability (Moeini et al., 2020). This observation could be seen in the SEM images, where less packed and high porosity morphology was observed in biocomposites. Despite the improvement in flexibility, less packed structure of biocomposites resulted from structural heterogeneity, and the reduced load-bearing capacity led to significant decrease in films stiffness from 1005.31 MPa in A/G20 to 103.64 MPa in Z/CH/GM:A/G20, and for the

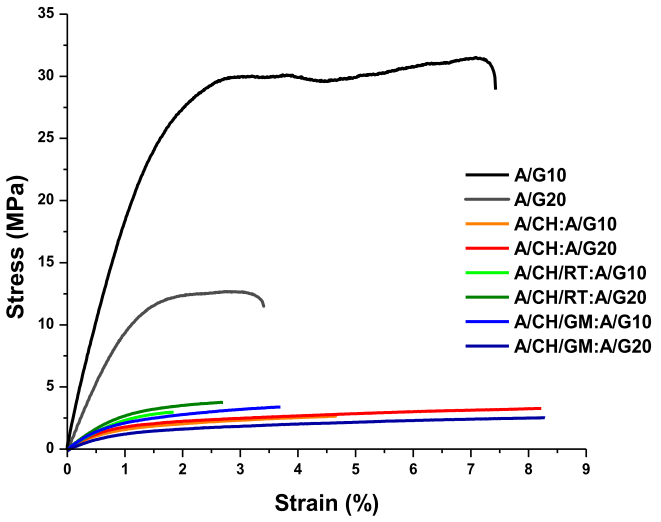

Fig. 7. Representative stress-strain curves of the alginate-based films.

same reason stress at break decreased from 21.67 MPa in A/G10 to 3.11 MPa in Z/CH:A/G10. In conclusion, A/G films are stiffer and stronger but less flexible. In contrast, biocomposite films with 20 % glycerol and encapsulated RT and GM are more flexible but weaker, making them adaptable for edible coating.

3.1.5. Water vapor barrier properties and surface wettability

The water vapor barrier properties of the alginate-based films are shown in Table 2. Alginate films are naturally highly permeable, with values like those reported for other polysaccharides, including chitosan and cellulose films and whey protein-based films (Agustin-Salazar et al., 2024; Arciello et al., 2021; Zhang et al., 2025). The addition of MPs and the natural extracts, RT and GM, did not cause the WVP values of the films to change dramatically. However, Z/CH/GM:A/G10 and Z/CH/RT:A/G20 showed the lowest permeability values, indicating that the interaction between matrix and MPs could be modulated by the incorporation of the natural extracts, leading to an increased tortuosity path for the water molecules diffusing within the film (Zhang et al., 2025).

Water contact angle measurements were employed to assess alginate-based films' hydrophilic or hydrophobic nature, directly influencing their interaction with water and other hydrophilic substances. Understanding these properties is critical for edible coatings, as surface wettability affects adhesion to food surfaces, moisture barrier performance, and overall coating functionality. As shown in Fig. 8, all alginate-based films exhibited a contact angle lower than 90°, as to confirm their hydrophilic nature. This property makes these films good candidates for edible coating application. Generally, the surface of films containing 20 % glycerol were more hydrophilic. Adding Z/CH, Z/CH/RT, and GM into films significantly increased the hydrophilicity, and the lowest contact angle was observed for Z/CH:A/G20 with 24.09° ± 6.94. Therefore, despite the more hydrophobic nature of chitosan and zein compared to alginate, the presence of embedded microparticles (MPs) caused contact angles to decrease. The main reasons for this finding are likely due to surface roughness of the samples. SEM analysis showed that films with MPs have a rougher and less homogeneous surface. Increased roughness can decrease the apparent contact angle, making the surface appear more wettable, as the roughness creates more surface area and micro/nano-scale voids where water can spread and penetrate, reducing the contact angle even if MPs are hydrophobic. Furthermore, clustering of MPs may favor the creation of microdomains of hydrophobicity surrounded by hydrophilic alginate, resulting in complex wetting behavior. Water droplets might preferentially wet the hydrophilic matrix areas, lowering the measured contact angle. Additionally, the presence of hydrophilic functional groups, predominantly distributed on the film surface, and the enhanced hydrogen bonding interactions confirmed by FTIR analysis contribute to this effect. Similar findings have been reported in several studies (Ali et al., 2014; Q. Li et al., 2020; Lin et al., 2010; Mayer et al., 2021). Besides, these results align well with the shelf-life test. They could confirm the effect of hydrophilicity on the tomato shelf-life extension, where a longer shelf life was observed in films with higher hydrophilicity. This can be due to the improved adhesion and uniform coverage on tomato surfaces in the films with a higher hydrophilic nature.

3.2. Biological assays and effect of alginate-based edible coating films on durability of tomatoes

3.2.1. Antioxidant activity (AA) of alginate films

The antioxidant properties of RT and GM extracts were estimated through a dose-dependent DPPH assay, resulting in a EC_{50} value, defined as the concentration of sample needed to reduce the DPPH concentration by 50 %, of 127,7 ± 1,6 μg/ml and 296,4 ± 5,1 μg/ml for RT and GM extract, respectively, which highlighted higher AA of RT compared to GM.

The AA of plain alginate films (A/G10 or G20), and films modified with unloaded MPs (Z/CH:A/G10 or G20) and loaded MPs (Z/CH/GM:A/G10 or G20, Z/CH/RT:A/G10 or G20) were also determined. The AA expressed per cm^2 of film during 168 h testing was negligible for the pristine alginate samples (Fig. 9). The biocomposite films displayed AA during the time-course experiment, with the lowest activity in the case of unloaded MP films, reaching about 40 % DPPH inhibition at the end of the experiment. The AA increased when GM extract was loaded in microparticles, achieving about 52 % DPPH inhibition. The highest AA was observed on film coated with RT-loaded MP, specifically in the case of Z/CH/RT:A/G20. The activity reached 70 % DPPH inhibition after 168h. This result agreed with the extended shelf life of tomatoes, up to 30 days, coated with the Z/CH/RT:A/G20 formulation (Fig. 9). In particular, Fig. 9 shows that Z/CH/RT:A/G20 reached the EC_{50} after 36 h, Z/CH/RT:A/G10 achieved the EC50 after 96 h, whereas the other films displayed the EC50 much later.

Our prior findings (data not shown) showed that red radish extract exhibited a higher AA than green mustard, mostly due to the higher total phenol content. Moreover, Park et al., 2019 reported that red radish showed the highest AA among 12 vegetable sprout species, which was highly correlated to the total phenol content (Park et al., 2019).

3.2.2. Antimicrobial assay

The survival of *Bacillus cereus* and *Salmonella enterica* was evaluated after 24 h of exposure to different alginate films. Antimicrobial activity was assessed on plain alginate films (A/G10 or A/G20), as well as films modified with unloaded microparticles (MPs) (Z/CH:A/G10 or A/G20) and MPs loaded with plant extracts (Z/CH/GM:A/G10 or A/G20; Z/CH/RT:A/G10 or A/G20). Among the tested coatings, the alginate film embedded with microparticles containing RT and 20 % glycerol (Z/CH/RT:A/G20) demonstrated the highest reduction in *B. cereus* survival, highlighting moderate antimicrobial properties (Fig. 10 A). In contrast, the alginate coating significantly reduced *S. enterica* vitality in the formulation containing unloaded MPs (Z/CH:A/G20) (Fig. 10 B). A further test was performed to assess the biocidal effect of chitosan as a constituent of the MPs. The antibacterial potential of pure chitosan film was further confirmed in *S. enterica*, as its survival was markedly reduced compared to polyvinyl alcohol (PVA) and PET (Fig. 10 C). Previous studies have demonstrated the ability of alginate and chitosan to control biofilm formation and microbial growth in Gram-positive and Gram-negative bacteria (Asadpoor et al., 2021; Dumont et al., 2018). The antimicrobial test in this study exhibited a certain degree of variability in biocidal action, which may be attributed to the need for direct bacterial contact with the coated surface (Mirbagheri et al., 2024). Additionally, this variability could contribute to potential inconsistencies in film preparation and the inability of chitosan or alginate

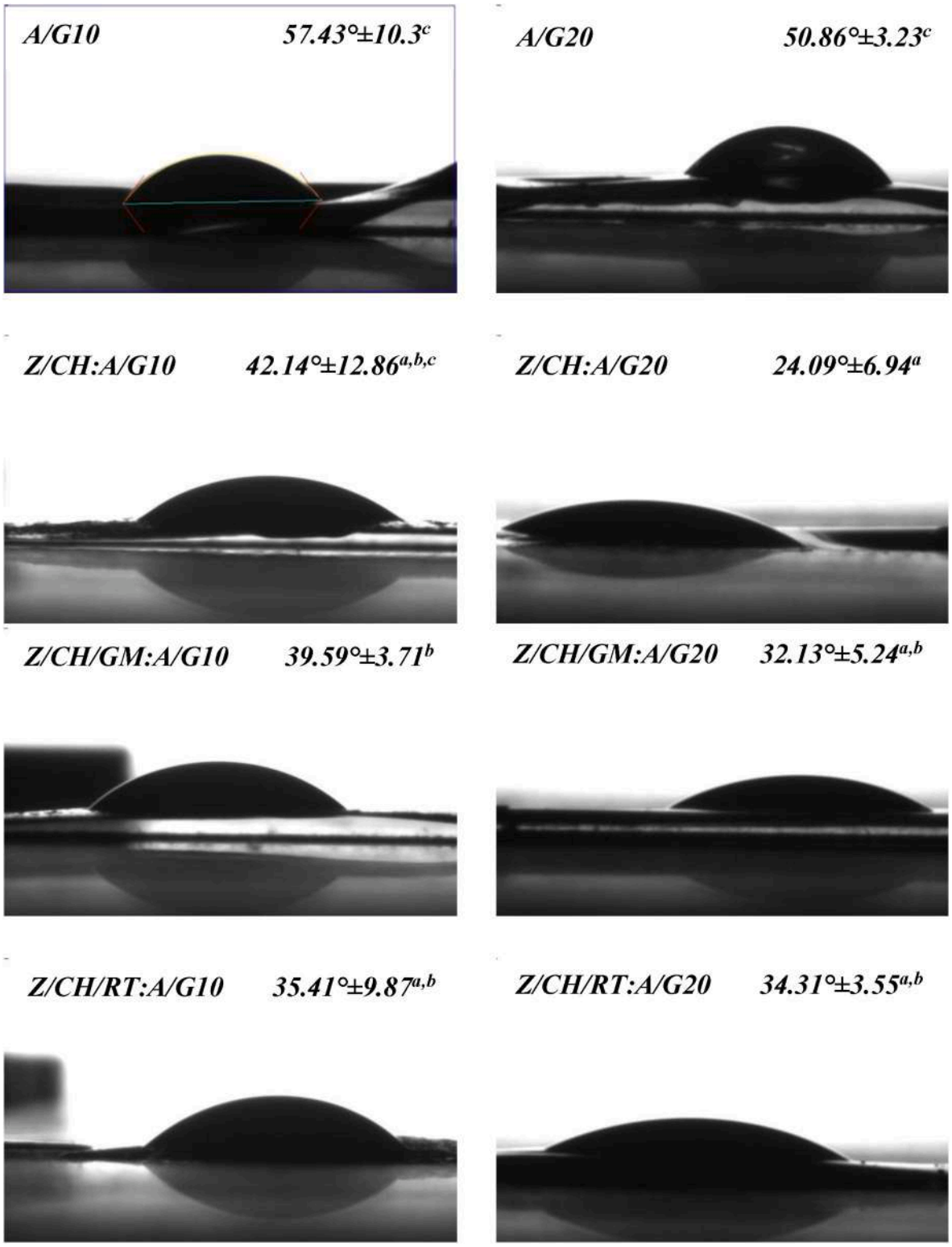

Fig. 8. Water Contact angle of A/G films and Z/CH, Z/CH/RT and GM:A/G biocomposites including alginate (A) and glycerol (G), green mustard (GM), red radish (RT), and microparticles (MPs) based on chitosan (CH) and zein (Z).

monomeric units to detach from the coating. We performed an agar diffusion assay with *S. enterica* and coatings containing pure chitosan to further investigate this. The absence of halos surrounding the chitosan-based biocomposite indicates that, according to this preliminary test, the films do not release diffusible chitosan (data not shown).

3.2.3. Application of developed Films for the preservation of durability of cherry tomatoes

A preliminary durability analysis was conducted on cherry tomatoes using a range of edible coatings solutions made from alginate, with varying concentrations of glycerol, microparticles, and encapsulated natural extracts (RT and GM) at room temperature (Fig. 11). The

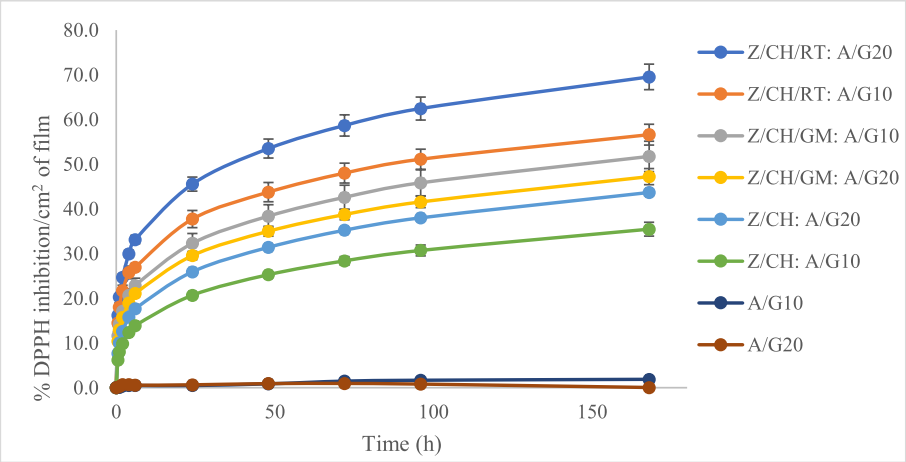

Fig. 9. Anti-oxidant assay of A/G films and Z/CH, Z/CH/RT and GM:A/G biocomposites for 7 days on DPPH. The samples include alginate (A) and glycerol (G), green mustard (GM), red radish (RT), and microparticles (MPs) based on chitosan (CH) and zein (Z). (For interpretation of the references to color in this figure legend, the reader is referred to the Web version of this article.)

research aimed to prolong the tomatoes' shelf life while preserving their quality and visual appeal, offering a different method to minimize post-harvest fruit and vegetable waste.

The uncoated tomatoes (control) stayed in good condition for 12 days. On day 8, a yellow spot emerged close to the green bud. By day 12, noticeable distortions and softening were visible, indicating the end of their suitability for sale, highlighting the quick decay of uncoated tomatoes under comparable storage conditions.

Tomatoes coated with Alginate containing 10 % glycerol (A/G10) exhibited visible deformation by day 12, making them unfit for sale. This coating formulation did not significantly extend the shelf life compared to the control, as the texture and firmness deteriorated at a similar pace. In A/G20, coated tomatoes showed a shelf life of 20 days; the visible deformations suggested that increasing glycerol concentration might have slowed the spoilage process, but did not wholly mitigate textural changes that could result from superior flexibility, moisture retention, and surface adhesion (Lindi et al., 2024). When microparticles were incorporated into the Alginate 10 % glycerol formulation (Z/CH: A/G10), the shelf life was extended to 27 days, though main issues with transparency and surface wrinkles were noted in the early days. Z/CH: A/G20 led to a shelf-life extension of 23 days; however, by day 23, significant wrinkles and deformations were observed, rendering the tomatoes unsalable. For tomatoes coated with Z/CH/GM: A/G10 and Z/CH/GM: A/G20, the shelf life was extended to day 23. However, careful optimization is crucial, as excessive glycerol could compromise barrier properties or encourage microbial growth. Despite the enhanced longevity, issues such as transparency loss, gradual softening, and surface texture wrinkles were observed, limiting the commercial potential of this formulation. These observations indicated that while GM extract helped extend the shelf life, it did not fully protect against surface deterioration in this formulation.

The Z/CH/RT: A/G10 extended the shelf life to day 20. By this point, the tomatoes displayed visible deformations and softening, indicating that while the coating delayed spoilage compared to the control, it did not entirely prevent the degradation of the product's texture and appearance. The most promising results were obtained with Alginate 20 % glycerol-containing encapsulated RT extract. This formulation extended the shelf life to 30 days, with no visible changes in appearance or texture until the final day of the study. This suggests that encapsulated RT, when combined with a higher glycerol concentration, can significantly improve the longevity and quality of tomatoes.

This study highlights the potential of using alginate-based edible films with encapsulated natural extracts for the shelf-life extension of tomatoes. Among the various formulations tested, Z/CH/RT:A/G20 showed the most significant improvement, extending the shelf life to 30 days without compromising appearance or texture. The success of this formulation can be attributed to its high antioxidant activity, derived from red radish extract (RT) properties, and the lower water vapor permeability. These properties work synergistically to combat moisture release, oxidative degradation, and microbial growth, which are key factors in tomato spoilage, thereby confirming the observed durability extension. For instance, the antioxidant activity, measured at 70 % DPPH inhibition, neutralizes free radicals that cause deterioration, while chitosan's antimicrobial action inhibits bacterial and fungal proliferation.

However, further studies on sensorial tests are needed to corroborate the shelf life tests further.

Fig. 12 presents the weight distribution of Alginate samples throughout 27 days. Every sample demonstrated a consistent weight reduction attributed to water loss through evaporation or various environmental factors. The control sample, devoid of any enhancements, exhibits a consistent linear weight loss throughout the storage duration, decreasing by about 8 %. This suggests a typical drying pattern without strategies to preserve moisture or impede water evaporation.

The highest weight loss was observed at A/G10, with 10.37 %, by day 23, significantly improving to 6.42 % at A/G20. This could be due to glycerol as a plasticizer, influencing moisture retention capabilities. The enhancement in the barrier properties could be seen in the biocomposite after the formulation of the MPs into the A polymer matrix, where the weight loss decreases from 10.37 % to 6.39 % in Z/CH:A/G10.

The best moisture retention of the samples was observed in the samples with RT, Z/CH/RT:A/G10, and Z/CH/RT:A/G20, with 6.06 % and 6.01 % after 27 days. This outcome aligns with other results, where better interaction between ingredients was found for RT formulated biocomposites, which also resulted in enhanced barrier properties of these biocomposite films.

4. Conclusions

In this study, we successfully developed an alginate-based active edible coating incorporating *Brassica juncea* (GM) and *Raphanus sativus* (RT) sprout extracts encapsulated in zein/chitosan (Z/CH) microparticles (MPs) and formulated into the alginate polymer matrix to extend the shelf life of tomatoes. The physicochemical characterization of the films demonstrated that the presence of MPs enhanced hydrophobization, reduced water absorption, and improved thermal stability while ensuring good dispersion and interaction within the polymer matrix. Tensile testing revealed that films with encapsulated RT and GM extracts

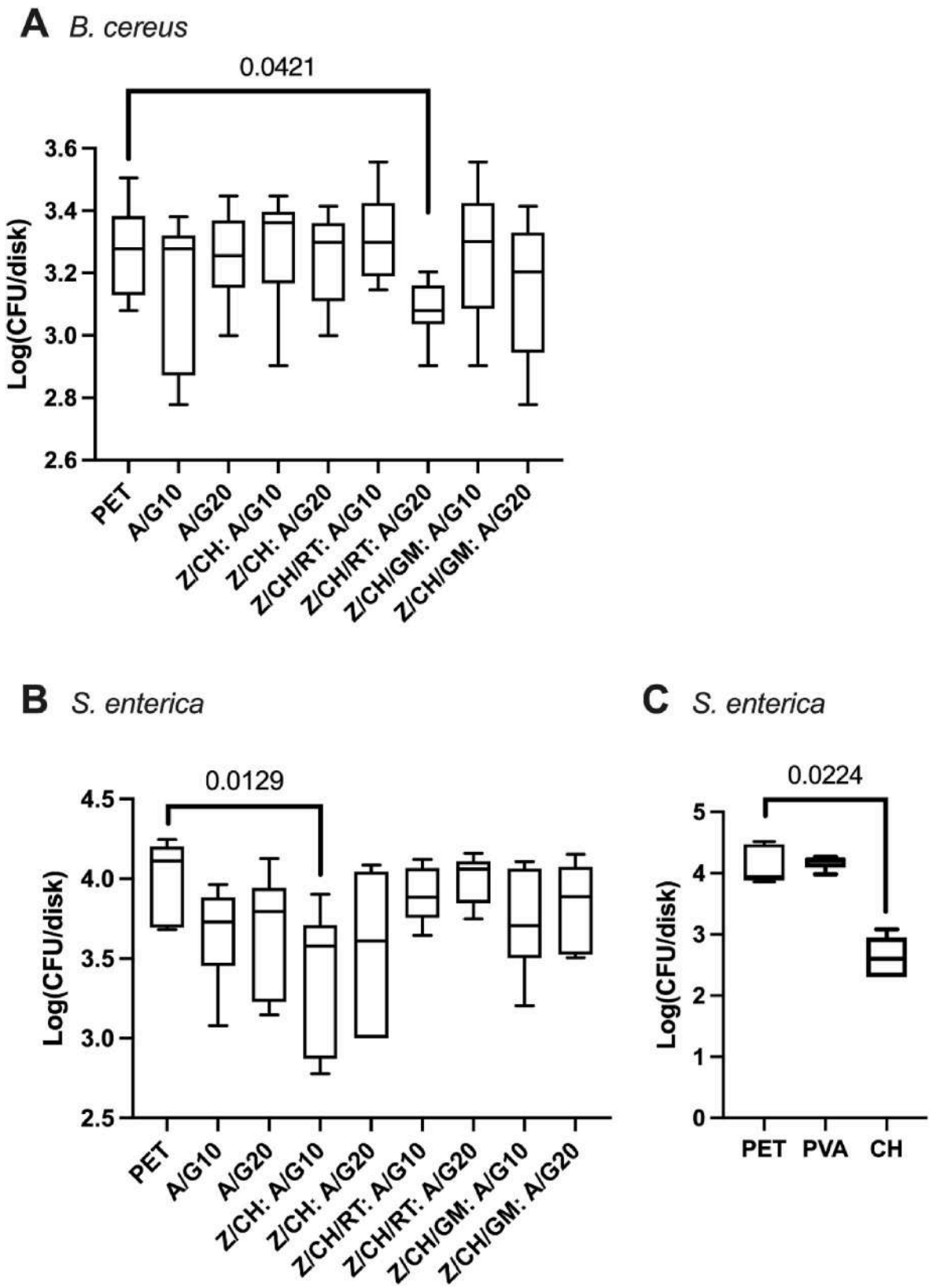

Fig. 10. Effect of different coating films on the survival of *Bacillus cereus* and *Salmonella enterica* after 24 h of exposure. (A) The survival of *B. cereus*, (B) the survival of *S. enterica*, (C) *S. enterica* survival on a chitosan film. Box plots represent the interquartile range, with thick lines indicating medians and whiskers showing data dispersion. Significant differences ($p < 0.05$) are indicated by numbers on the horizontal bars. Film types include polyethylene terephthalate (PET), and alginate (A) films containing green mustard (GM), red radish (RT), and microparticles (MP) based on chitosan (CH) and zein (Z). *S. enterica* was tested on chitosan (CH) and polyvinyl alcohol (PVA) as a control.

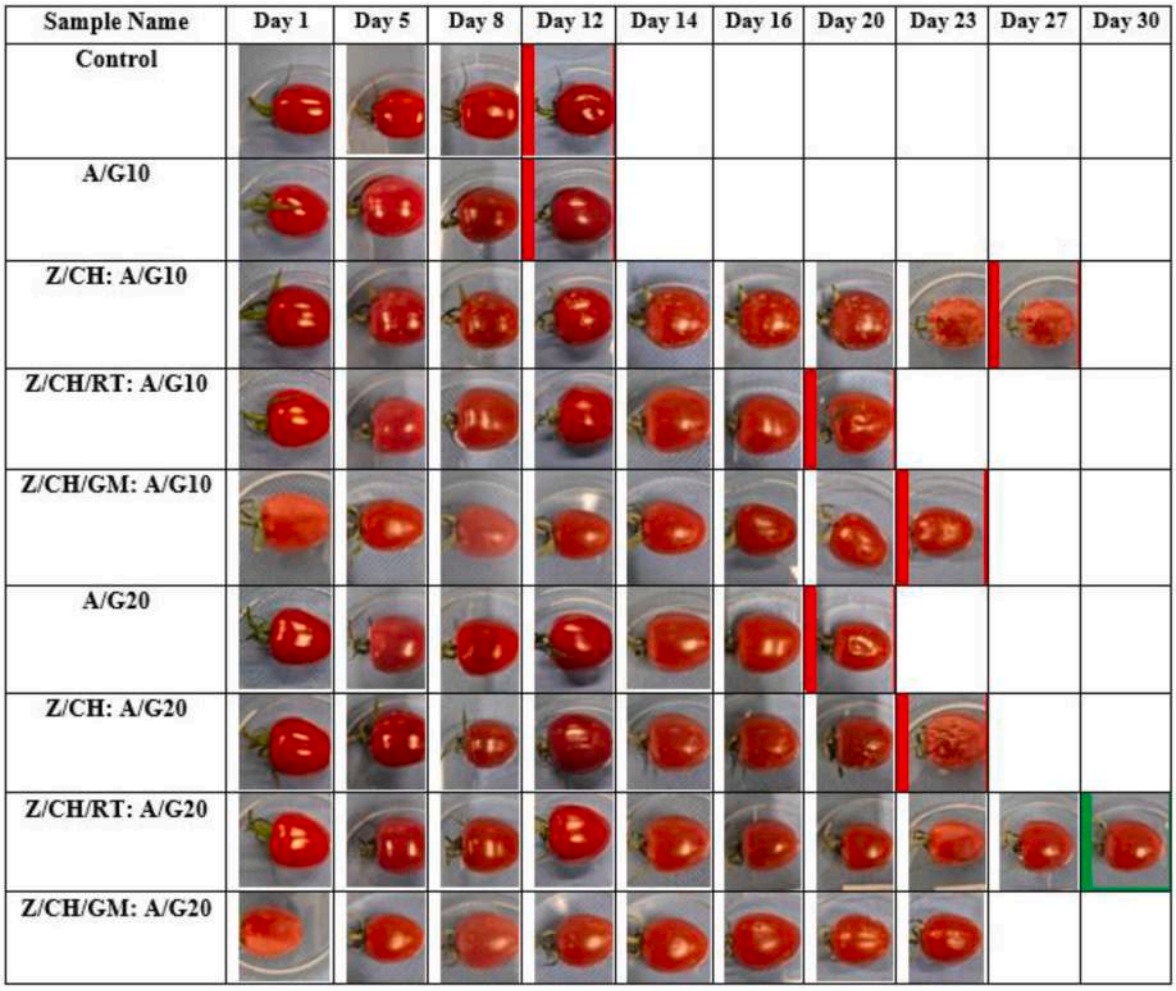

Fig. 11. Storage test of uncoated and coated cherry tomatoes. Coating types include alginate (A) and glycerol (G), green mustard (GM), red radish (RT), and microparticles (MPs) based on chitosan (CH) and zein (Z). A/G10 and A/G20 as the control and Z/CH/RT:A/G10, Z/CH/RT:A/G20, Z/CH/GM:A/G10 and Z/CH/GM:A/G20 for 30 days at room temperature. (For interpretation of the references to color in this figure legend, the reader is referred to the Web version of this article.)

were more flexible, making them ideal for use as edible coatings. The antioxidant activity of the films was significantly enhanced by the inclusion of GM and RT extracts, with the RT-loaded films showing the highest DPPH inhibition. Tomatoes coated with the Z/CH/RT:A/G20 formulation exhibited an extended shelf life of up to 30 days without visible deterioration in appearance or texture, confirming the coating's effectiveness. Additionally, these films demonstrated the highest biocidal activity against *Bacillus cereus* and *Salmonella enterica*, highlighting their potential for food safety applications.

Beyond the technical performance, this approach is also aligned with principles of sustainability and circularity. Using natural, biodegradable polymers such as alginate, chitosan, and plant-based extracts reduces the environmental impact of food packaging. The potential for utilizing sprout extracts in the formulation further supports a circular economy by adding value to these fast-growing renewable sources. This work highlights the potential for environmentally friendly, bioactive coatings that improve food preservation while reducing reliance on synthetic preservatives, offering an effective and sustainable solution for fresh produce storage. Future research can focus on scaling up the formulation, optimizing bioactive compound concentrations, and exploring its application to other fruits and vegetables, enhancing the approach's scope, circularity, and sustainability.

CRediT authorship contribution statement

Arash Moeini: Writing – review & editing, Writing – original draft, Validation, Supervision, Resources, Project administration, Methodology, Investigation, Funding acquisition, Conceptualization. **Sarai Agustin Salazar:** Writing – review & editing, Writing – original draft, Visualization, Validation, Investigation, Formal analysis. **Luca Gargiulo:** Writing – original draft, Validation, Formal analysis. **Roméo Arago Dougué Kentsop:** Writing – review & editing, Writing – original draft, Visualization, Validation, Formal analysis, Conceptualization. **Monica Mattana:** Writing – original draft, Validation, Supervision, Resources, Project administration, Funding acquisition, Conceptualization. **Annamaria Genga:** Writing – review & editing, Supervision, Conceptualization. **Christin Josi:** Writing – original draft, Investigation, Formal analysis. **Parisa Pedram:** Writing – review & editing, Visualization, Investigation. **Gustavo Cabrera-Barjas:** Writing – review & editing. **Simona Guerra:** Writing – original draft, Formal analysis. **Massimiliano Marvasi:** Writing – review & editing, Writing – original draft, Validation, Methodology, Investigation, Formal analysis. **Thomas Becker:** Writing – review & editing, Supervision, Project administration. **Pierfrancesco Cerruti:** Writing – review & editing, Validation, Supervision, Project administration, Methodology, Funding acquisition.

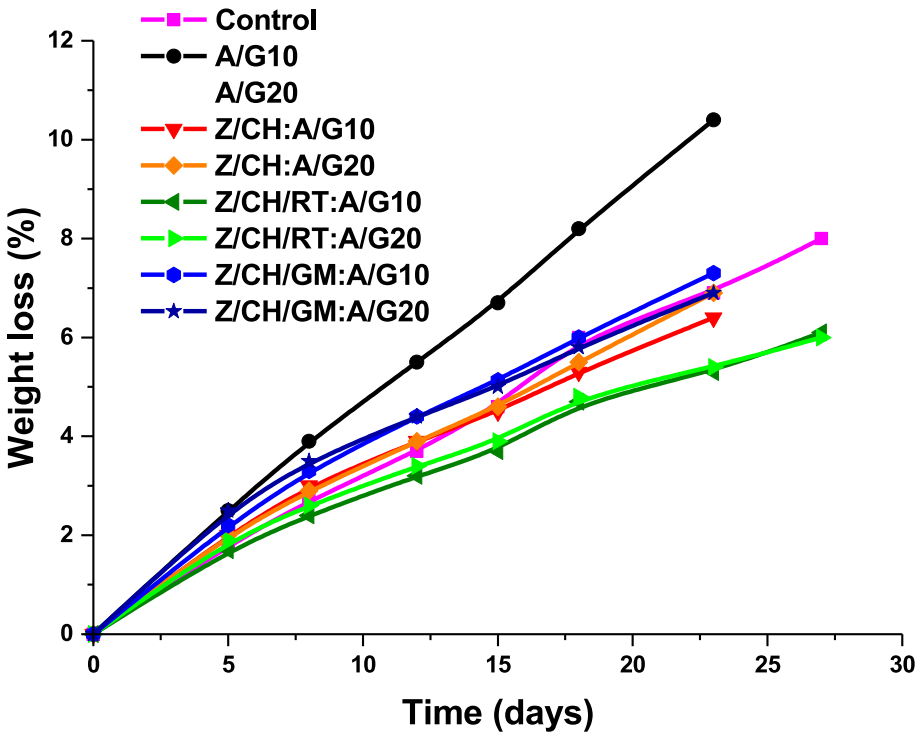

Fig. 12. Samples' weight loss percentage (%) over the storage period of uncoated and coated cherry tomatoes. Coating types include alginate (A) and glycerol (G), green mustard (GM), red radish (RT), and microparticles (MPs) based on chitosan (CH) and zein (Z). A/G10 and A/G20 as the control and Z/CH/RT:A/G10, Z/CH/RT:A/G20, Z/CH/GM:A/G10 and Z/CH/GM:A/G20 for 30 days at room temperature. (For interpretation of the references to color in this figure legend, the reader is referred to the Web version of this article.)

Declaration of competing interest

The authors declare the following financial interests/personal relationships which may be considered as potential competing interests:

Arash Moeini reports financial support was provided by EU Horizon 2020 PRIMA. If there are other authors, they declare that they have no known competing financial interests or personal relationships that could have appeared to influence the work reported in this paper.

Acknowledgment

The European Union's Horizon 2020 research and innovation program (PRIMA call) funded the current work under grant agreement No. 02WPM1683, EU Project, "From Edible Sprouts to hEalthy food (FEED)."

Appendix A. Supplementary data

Supplementary data to this article can be found online at https://doi.org/10.1016/j.foodhyd.2025.111693.

Data availability

Data will be made available on request.

References

Agustin-Salazar, S., Gámez-Meza, N., Medina-Juárez, L. A., Malinconico, M., & Cerruti, P. (2017). Stabilization of polylactic acid and polyethylene with Nutshell extract: Efficiency assessment and economic evaluation. *ACS Sustainable Chemistry & Engineering, 5*. https://doi.org/10.1021/acssuschemeng.6b03124

Agustin-Salazar, S., Torrieri, E., Immirzi, B., & Di Lorenzo, M. L. (2024a). Cellulose-based sustainable packaging of leafy vegetables: An experimental study on the shelf life of baby spinach. *Organic Agriculture, 14*(2), 167–180. https://doi.org/10.1007/s13165-023-00450-5

Agustin-Salazar, S., Torrieri, E., Immirzi, B., & Di Lorenzo, M. L. (2024b). Cellulose-based sustainable packaging of leafy vegetables: An experimental study on the shelf life of baby spinach. *Organic Agriculture, 14*(2), 167–180. https://doi.org/10.1007/s13165-023-00450-5

Ali, S., Khatri, Z., Oh, K. W., Kim, I.-S., & Kim, S. H. (2014). Zein/cellulose acetate hybrid nanofibers: Electrospinning and characterization. *Macromolecular Research, 22*(9), 971–977. https://doi.org/10.1007/s13233-014-2136-4

Asadpoor, M., Ithakisiou, G.-N., van Putten, J. P. M., Pieters, R. J., Folkerts, G., & Braber, S. (2021). Antimicrobial activities of alginate and chitosan oligosaccharides against Staphylococcus aureus and Group B streptococcus. *Frontiers in Microbiology, 12*. https://www.frontiersin.org/journals/microbiology/articles/10.3389/fmicb.2021.700605.

Aspen, B. (2024). *Encapsulation of novel natural compounds for the development of active edible coating applications*. Munich: Technical University of.

Astm, E. (2014). *Standard Test methods for water vapor transmission of materials*. U.S. Department of Defense. www.astm.org.

Bahraminejad, S., Mousavi, M., Askari, G., & Gharaghani, M. (2023). Effect of octenylsuccination of alginate on structure, mechanical and barrier properties of alginate-zein composite film. *International Journal of Biological Macromolecules, 226*, 463–472. https://doi.org/10.1016/j.ijbiomac.2022.12.019

Chien, P.-J., Sheu, F., & Yang, F.-H. (2007). Effects of edible chitosan coating on quality and shelf life of sliced mango fruit. *Journal of Food Engineering, 78*(1), 225–229. https://doi.org/10.1016/j.jfoodeng.2005.09.022

Communication from the Commission to the European Parliament, the Council. (2015). *The European Economic and Social Committee and the Committee of the Regions closing the loop - An EU action plan for the circular economy*. Brussels, Belgium: European Commission. __ https://eur-lex.europa.eu/legal-content/EN/TXT/?uri=CELEX:52015DC0614.

Derkach, S. R., Voron'ko, N. G., Sokolan, N. I., Kolotova, D. S., & Kuchina, Y. A. (2020). Interactions between gelatin and sodium alginate: UV and FTIR studies. *Journal of Dispersion Science and Technology, 41*(5), 690–698. https://doi.org/10.1080/01932691.2019.1611437

Di Donato, P., Taurisano, V., Poli, A., Gomez d'Ayala, G., Nicolaus, B., Malinconinco, M., & Santagata, G. (2020). Vegetable wastes derived polysaccharides as natural eco-friendly plasticizers of sodium alginate. *Carbohydrate Polymers, 229*, Article 115427. https://doi.org/10.1016/j.carbpol.2019.115427

Dumont, M., Villet, R., Guirand, M., Montembault, A., Delair, T., Lack, S., Barikosky, M., Crepet, A., Alcouffe, P., Laurent, F., & David, L. (2018). Processing and antibacterial properties of chitosan-coated alginate fibers. *Carbohydrate Polymers, 190*, 31–42. https://doi.org/10.1016/j.carbpol.2017.11.088

Gao, C., Pollet, E., & Avérous, L. (2017). Properties of glycerol-plasticized alginate films obtained by thermo-mechanical mixing. *Food Hydrocolloids, 63*, 414–420. https://doi.org/10.1016/j.foodhyd.2016.09.023

Garcia, C. C., Caetano, L. C., de Souza Silva, K., & Mauro, M. A. (2014). Influence of edible coating on the drying and quality of papaya (Carica papaya). *Food and Bioprocess Technology, 7*(10), 2828–2839. https://doi.org/10.1007/s11947-014-1350-6

Giannakas, A. E., Salmas, C. E., Moschovas, D., Zaharioudakis, K., Georgopoulos, S., Asimakopoulos, G., Aktypis, A., Proestos, C., Karakassides, A., Avgeropoulos, A., Zafeiropoulos, N. E., & Nychas, G. J. (2022). The increase of soft cheese shelf-life packaged with edible films based on novel hybrid nanostructures. *Gels, 8*(9). https://doi.org/10.3390/gels8090539

Giannakas, A. E., Zaharioudakis, K., Kollia, E., Kopsacheili, A., Avdylaj, L., Georgopoulos, S., Leontiou, A., Karabagias, V. K., Kehayias, G., Ragkava, E., Proestos, C., & Salmas, C. E. (2023). The development of a novel sodium alginate-based edible active Hydrogel coating and its application on traditional Greek spreadable cheese. *Gels, 9*(10). https://doi.org/10.3390/gels9100807

Gonçalves, S. M., dos Santos, D. C., Motta, J. F. G., Santos, R. R. dos, Chávez, D. W. H., & Melo, N. R. de (2019). Structure and functional properties of cellulose acetate films incorporated with glycerol. *Carbohydrate Polymers, 209*, 190–197. https://doi.org/10.1016/j.carbpol.2019.01.031

Goyeneche, R., Roura, S., Ponce, A., Vega-Gálvez, A., Quispe-Fuentes, I., Uribe, E., & Di Scala, K. (2015). Chemical characterization and antioxidant capacity of red radish (Raphanus sativus L.) leaves and roots. *Journal of Functional Foods, 16*, 256–264. https://doi.org/10.1016/j.jff.2015.04.049

Granato, D., Nunes, D. S., & Barba, F. J. (2017). An integrated strategy between food chemistry, biology, nutrition, pharmacology, and statistics in the development of functional foods: A proposal. *Trends in Food Science & Technology, 62*, 13–22. https://doi.org/10.1016/j.tifs.2016.12.010

Horita, C. N., Baptista, R. C., Caturla, M. Y. R., Lorenzo, J. M., Barba, F. J., & Sant'Ana, A. S. (2018). Combining reformulation, active packaging and non-thermal post-packaging decontamination technologies to increase the microbiological quality and safety of cooked ready-to-eat meat products. *Trends in Food Science & Technology, 72*, 45–61. https://doi.org/10.1016/j.tifs.2017.12.003

Ioannou, E., & Roussis, V. (2009). Natural products from seaweeds. *springerLink*, 51–81. https://doi.org/10.1007/978-0-387-85498-4_2

Johnson, J. L., Raghavan, V., Cimmino, A., Moeini, A., Petrovic, A. G., Santoro, E., Superchi, S., Berova, N., Evidente, A., & Polavarapu, P. L. (2018). Absolute configurations of chiral molecules with multiple stereogenic centers without prior knowledge of the relative configurations: A case study of inuloxin C. *Chirality, 30*(11). https://doi.org/10.1002/chir.23013

Jost, V., Kobsik, K., Schmid, M., & Noller, K. (2014). Influence of plasticiser on the barrier, mechanical and grease resistance properties of alginate cast films. *Carbohydrate Polymers, 110*, 309–319. https://doi.org/10.1016/j.carbpol.2014.03.096

Li, Q., Gao, R., Wang, L., Xu, M., Yuan, Y., Ma, L., Wan, Z., & Yang, X. (2020). Nanocomposites of bacterial cellulose nanofibrils and zein nanoparticles for food packaging. *ACS Applied Nano Materials, 3*(3), 2899–2910. https://doi.org/10.1021/acsanm.0c00159

Li, Y., Lu, J., Tian, X., Xu, Z., Huang, L., Xiao, H., Ren, X., & Kong, Q. (2021). Alginate with citrus pectin and pterostilbene as healthy food packaging with antioxidant property. *International Journal of Biological Macromolecules, 193*, 2093–2102. https://doi.org/10.1016/j.ijbiomac.2021.11.041

Lin, Y.-J., Cai, Q., Li, Q.-F., Xue, L.-W., Jin, R.-G., & Yang, X.-P. (2010). Effect of solvent on surface wettability of electrospun polyphosphazene nanofibers. *Journal of Applied Polymer Science, 115*(6), 3393–3400. https://doi.org/10.1002/app.30481

Lindi, A. M., Gorgani, L., Mohammadi, M., Hamedi, S., Darzi, G. N., Cerruti, P., Fattahi, E., & Moeini, A. (2024). Fenugreek seed mucilage-based active edible films for extending fresh fruit shelf life: Antimicrobial and physicochemical properties. *International Journal of Biological Macromolecules, 269*, Article 132186. https://doi.org/10.1016/j.ijbiomac.2024.132186

Liu, Y., Li, S., Li, H., Alomgir Hossen, M., Sameen, D. E., Dai, J., Qin, W., & Lee, K. (2021). Synthesis and properties of core-shell thymol-loaded zein/shellac nanoparticles by coaxial electrospray as edible coatings. *Materials & Design, 212*, Article 110214. https://doi.org/10.1016/j.matdes.2021.110214

Mayer, S., Tallawi, M., De Luca, I., Calarco, A., Reinhardt, N., Gray, L. A., Drechsler, K., Moeini, A., & Germann, N. (2021). Antimicrobial and Physicochemical characterization of 2,3 Dialdehyde cellulose-based wound dressings systems. *Carbohydrate Polymers*. , Article 118506.. https://doi.org/10.1016/j.carbpol.2021.118506

Meng, X., Li, B., Liu, J., & Tian, S. (2008). Physiological responses and quality attributes of table grape fruit to chitosan preharvest spray and postharvest coating during storage. *Food Chemistry, 106*(2), 501–508. https://doi.org/10.1016/j.foodchem.2007.06.012

Meseldzija, S., Ruzic, J., Spasojevic, J., Momcilovic, M., Moeini, A., Cabrera-Barjas, G., & Nesic, A. (2024). Alginate cryogels as a template for the preparation of edible oleogels. *Foods, 13*(Issue 9). https://doi.org/10.3390/foods13091297

Mirbagheri, V. S., Alishahi, A., Ahmadian, G., Hashemi Petroudi, S. H., Ojagh, S. M., & Romanazzi, G. (2024). Toward understanding the antibacterial mechanism of chitosan: Experimental approach and in silico analysis. *Food Hydrocolloids, 147*, Article 109382. https://doi.org/10.1016/j.foodhyd.2023.109382

Moccia, F., Agustin-Salazar, S., Berg, A.-L., Setaro, B., Micillo, R., Pizzo, E., Weber, F., Gamez-Meza, N., Schieber, A., Cerruti, P., Panzella, L., & Napolitano, A. (2020). Pecan (Carya illinoinensis (Wagenh.) K. Koch) Nut shell as an accessible polyphenol source for active packaging and food colorant stabilization. *ACS Sustainable Chemistry & Engineering, 8*(17), 6700–6712. https://doi.org/10.1021/acssuschemeng.0c00356

Moeini, A. (2020). *Fungal and plant metabolites formulated into biopolymers, with anti-mold activity for food packaging*. University of Naples Federico II.

Moeini, A., Cimmino, A., Dal Poggetto, G., Di Biase, M., Evidente, A., Masi, M., Lavermicocca, P., Valerio, F., Leone, A., Santagata, G., & Malinconico, M. (2018). Effect of pH and TPP concentration on chemico-physical properties, release kinetics and antifungal activity of Chitosan-TPP-Ungeremine microbeads. *Carbohydrate Polymers, 195*, 631–641. https://doi.org/10.1016/j.carbpol.2018.05.005

Moeini, A., Mallardo, S., Cimmino, A., Dal Poggetto, G., Masi, M., Di Biase, M., van Reenen, A., Lavermicocca, P., Valerio, F., Evidente, A., Malinconico, M., & Santagata, G. (2020). Thermoplastic starch and bioactive chitosan sub-microparticle biocomposites: Antifungal and chemico-physical properties of the films. *Carbohydrate Polymers, 230*. https://doi.org/10.1016/j.carbpol.2019.115627

Moeini, A., Pedram, P., Makvandi, P., Malinconico, M., & Gomez d'Ayala, G. (2020). Wound healing and Antimicrobial effect of active Secondary Metabolites in Chitosan-based wound dressings: A review. *Carbohydrate Polymers*. , Article 115839.. https://doi.org/10.1016/j.carbpol.2020.115839

Moeini, A., van Reenen, A., Van Otterlo, W., Cimmino, A., Masi, M., Lavermicocca, P., Valerio, F., Immirzi, B., Santagata, G., Malinconico, M., & Evidente, A. (2020). α-costic acid, a plant sesquiterpenoid from Dittrichia viscosa, as modifier of Poly (lactic acid) properties: A novel exploitation of the autochthone biomass metabolite for a wholly biodegradable system. *Industrial Crops and Products, 146*. https://doi.org/10.1016/j.indcrop.2020.112134

Mohammadi, M., Mirabzadeh, S., Shahvalizadeh, R., & Hamishehkar, H. (2020). Development of novel active packaging films based on whey protein isolate incorporated with chitosan nanofiber and nano-formulated cinnamon oil. *International Journal of Biological Macromolecules, 149*, 11–20. https://doi.org/10.1016/j.ijbiomac.2020.01.083

Mohan, S., Unnikrishnan, T. G., Dubey, U., Ramesh, M., & Panneerselvam, K. (2023). Development and characterization of mustard oil incorporated biodegradable chitosan films for active food packaging applications. *Journal of Polymers and the Environment, 31*(5), 2190–2203. https://doi.org/10.1007/s10924-022-02719-4

Nesic, A., Moeini, A., & Santagata, G. (2020). Marine biopolymers: Alginate and chitosan. In P. C. Valentina Marturano, & V. Ambrogi (Eds.), *Sustainability of polymeric materials* (p. 73). De Gruyter. https://doi.org/10.1515/9783110590586-004.

Nguyen Van Long, N., Joly, C., & Dantigny, P. (2016). Active packaging with antifungal activities. *International Journal of Food Microbiology, 220*, 73–90. https://doi.org/10.1016/j.ijfoodmicro.2016.01.001

No, H. K., Meyers, S. P., & Prinyawiwatkul, W. (2007). Applications of chitosan for improvement of quality and Shelf life of foods: A review. *Journal of Food Science, 72*, R87–R100. https://doi.org/10.1111/j.1750-3841.2007.00383.x

Padua, G., & Wang, Q. (2002). Formation and properties of corn zein films and coatings. In *Protein-Based films and coatings*. https://doi.org/10.1201/9781420031980.ch2

Park, H., Shin, Y., & Kim, Y. J. (2019). Antioxidant contents and activities of twelve varieties of vegetable sprouts. *Korean Journal of Food Science and Technology, 51*(3), 207–213. https://doi.org/10.9721/KJFST.2019.51.3.207

Sahraee, S., Milani, J. M., Regenstein, J. M., & Kafil, H. S. (2019). Protection of foods against oxidative deterioration using edible films and coatings: A review. *Food Bioscience, 32*, Article 100451. https://doi.org/10.1016/j.fbio.2019.100451

Spasojević, L., Katona, J., Bučko, S., Savić, S. M., Petrović, L., Milinković Budinčić, J., Tasić, N., Aidarova, S., & Sharipova, A. (2019). Edible water barrier films prepared from aqueous dispersions of zein nanoparticles. *LWT, 109*, 350–358. https://doi.org/10.1016/j.lwt.2019.04.038

Szőllősi, R. (2020). Chapter 25 - Indian mustard (Brassica juncea L.) seeds in health. In V. R. Preedy, & R. R. Watson (Eds.), *Nuts and seeds in health and disease prevention* (2nd ed., pp. 357–364). Academic Press. https://doi.org/10.1016/B978-0-12-818553-7.00025-5.

Theagarajan, R., Dutta, S., Moses, J. A., & Chinnaswamy, A. (2019). *Alginates for Food Packaging Applications*, 205–232. https://doi.org/10.1002/9781119487999.ch11

Valdés, A., Mellinas, A. C., Ramos, M., Garrigós, M. C., & Jiménez, A. (2014). Natural additives and agricultural wastes in biopolymer formulations for food packaging. *Frontiers in Chemistry, 2*(6). https://www.frontiersin.org/article/10.3389/fchem.2014.00006.

Vinceković, M., Viskić, M., Jurić, S., Giacometti, J., Bursać Kovačević, D., Putnik, P., Donsì, F., Barba, F. J., & Režek Jambrak, A. (2017). Innovative technologies for encapsulation of Mediterranean plants extracts. *Trends in Food Science & Technology, 69*, 1–12. https://doi.org/10.1016/j.tifs.2017.08.001